TIME-DEPENDENT BEHAVIOR OF VARIOUS FRP COMPOSITES FOR

STRUCTURAL APPLICATIONS

A Thesis
Submitted to the Graduate Faculty
of the
North Dakota State University
of Agriculture and Applied Science

By

Md. Fuad Hassan Khan

In Partial Fulfillment of the Requirements
for the Degree of
MASTER OF SCIENCE

Major Department:
Civil Engineering

July 2011

Fargo, North Dakota

North Dakota State University
Graduate School

Title

TIME-DEPENDENT BEHAVIOR OF VARIOUS FRP

COMPOSITES FOR STRUCTURAL APPLICATIONS

By

Md. Fuad Hassan Khan

The Supervisory Committee certifies that this *disquisition* complies with North Dakota State University's regulations and meets the accepted standards for the degree of

MASTER OF SCIENCE

ABSTRACT

Khan, Md. Fuad Hassan, M.S., Department of Civil Engineering, College of Engineering and Architecture, North Dakota State University, July 2011. Time-dependent Behavior of Various FRP Composites for Structural Applications. Major Professor: Dr. Yail Jimmy Kim.

This thesis represents the long-term behavior of fiber reinforced polymer (FRP) materials for structural applications. FRP composites consist of high-strength fibers embedded in an epoxy resin. The long-term investigations include i) pultruded glass FRP (GFRP) beams subjected to sustained loads and cold temperature and ii) reinforced concrete beams strengthened with near-surface mounted (NSM) carbon FRP (CFRP) strips. For the first phase, test parameters include the variation of sustained intensities and temperature. The flexural behavior of the long-term beams is studied through a combined experimental and numerical approach, including load-carrying capacity, failure mode, creep response, and material degradation. Some material parameters that are crucial for practical applications are suggested using a regression analysis. A finite element model is developed to predict the behavior of GFRP beams. An analytical model is also proposed to estimate the long-term behavior of GFRP composites for structural applications. For the second phase, test parameters include the variation of sustained intensities, CFRP strengthening schemes and bonding agents. The short-term beams are loaded both monotonically and cyclically whereas the long-term beams are loaded only monotonically. The flexural behavior of all beams is studied through an experimental investigation, including load-carrying capacity, failure mode, creep response, and material degradation.

ACKNOWLEDGEMENTS

This work would have never been completed without the guidance and support of many individuals. "Thank you" will never express my full gratitude for these people, but I assure each and every one of them that I shall never forget, and forever I will be grateful for all I have learned from each of them.

TABLE OF CONTENTS

LIST OF TABLES

LIST OF FIGURES

NOTATIONS

A Cross sectional area

a Distance from support to loading point

b_f Flange width

C_b Moment coefficient

C_w Wraping coefficient

D_L Plate rigidities in longitudinal directions

D_{LT} Plate flexural rigidities in longitudinal and transverse directions

D_s Shear rigidities

D_T Plate rigidities in transverse directions

d_w Depth of web

E_c Concrete modulus

E_c^L Longitudinal compressive modulus

E_c^T Transverse compressive modulus

E_i Initial modulus of GFRP beam

E_L Longitudinal modulus

E_r Residual modulus

E_t Time-depended modulus

E_t^L Longitudinal tensile modulus

E_t^T Transverse tensile modulus

E_v Visco-elatic modulus of GFRP beam

G Shear modulus

G_{LT} Longitudinal shear modulus

I	Moment of inertia
I_e	Effective moment of inertia
I_y	Moment of inertia in week axis
J	Polar moment of inertia
K	Shear coefficient
K_f	Flange end retrained coefficient
k_{LT}	Shear buckling coefficient
K_w	Web end restrained coefficient
L	Span length
l	Span length
L_b	Beam span length
m	GFRP creep parameter
n	GFRP creep parameter
P	Applied load
P_u	Ultimate load
S_x	Section modulus
T	Plate thickness
t	Time
t_f	Flange thickness
t_i	Initial time
t_w	Thickness of web
β	Materials constant
δ	Mid-span deflection
ε	Time-depended strain

ε_i	Visco-elastic strain
ε_L^{fu}	Tensile rupture strain
ζ	Non dimensional restrained coefficient
Π	Constant(Pie)
σ	Applied constant stress
σ_c^L	Longitudinal compressive strength
σ_{cr}^{flange}	Critical stress for flange buckling
σ_{cr}^{LTB}	Critical stress for lateral torsional buckling
σ_{cr}^{web}	Critical stress for web buckling of the section
σ_c^T	Transverse compressive strength
σ_t^L	Longitudinal tensile strength
σ_t^T	Transverse tensile strength
τ_{cr}^{web}	Critical shear stress in web
υ_L	Poisson's ratio in longitudinal directions
υ_T	Poisson's ratio in transverse directions

CHAPTER 1. INTRODUCTION

1.1. GENERAL

Aging and decaying of U.S. infrastructure require urgent attention. The necessity of travel diversity is placing greater demand for enhanced transportation systems and public services. According to the American Society of Civil Engineers (ASCE 2009) Infrastructure Report Card, the infrastructure of the USA is given a grade of "D", which is a critical state across all categories such as bridges, dams and roads. Further, ASCE estimates that the five-year needed investment to address the USA's deficient infrastructure is $2.2 trillion. To put this in perspective, the present national shortage is approximately $14 trillion, and yet we need $2.2 trillion to keep the infrastructure intact, safe and contributing to economic growth. The inadequate condition of roads, rails, ports and air transport networks has been noted by different key international organizations. According to the 2010–2011 Global Competitiveness Index published by the World Economic Forum, the USA ranked 15th in the category of infrastructure. This ranking would seem to be the direct byproduct of a 50% decline in U.S. infrastructure investment as a percentage of Gross Domestic Product since 1960. From a survey on bridges collapsed in USA it was found that almost 50% of the bridges collapsed in USA (Wikipedia list of bridge failures 2009) were because of fatigue failure, poor construction, material fault and corrosion, over load (increased traffic loads), weak joint, undersized gusset plates and deterioration. It has become an imperative action to reconstruct or rehabilitate deficient structures for the safety of the public.

Top three infrastructure concerns in North Dakota are roads, wastewater and bridges. 22% of North Dakota's bridges are structurally deficient or functionally obsolete

(ASCE report card 2009). There are 29 high hazard dams in North Dakota. A high hazard dam is defined as a dam whose failure would cause a loss of life and significant property damage. Eighteen of North Dakota's 1,150 dams are in need of rehabilitation to meet applicable state dam safety standards. 45% of high hazard dams in North Dakota have no emergency action plan (EAP). An EAP is a predetermined plan of action to be taken including roles, responsibilities and procedures for surveillance, notification, and evacuation to reduce the potential for loss of life and property damage in an area affected by a failure or mis-operation of a dam. North Dakota reported an unmet need of $3.7 million for its state public outdoor recreation facilities and parkland acquisition. 25% of North Dakota's major roads are in poor or mediocre condition. Vehicle travel on North Dakota's highways increased 47% from 1990 to 2007.

Congested highways, overflowing sewers and corroding bridges are constant reminders of the looming crisis that jeopardizes the nation's prosperity and quality of life. It is the infrastructure action time and establishing a long-term development and maintenance plan must become a national priority. For raising the grade of America's infrastructures, it needs lots of money, lots of time, and lots of commitment. Although the efforts taken last decades show some improvement for the bridges of rural areas, the condition of the bridges at urban areas has been declined by this time. A number of factors influence the service life of structures, such as increased traffic loads, aging, corrosion, sulfate attack, cold temperature, and impact damage (Enright and Frangopol 2000; Shahrooz et al. 2002). In 2007 when I-35 Bridge (which was classified as structurally deficient or functionally obsolete by ASCE 2005 report) collapsed in Minneapolis, the tragedy reverberated throughout the nation; the collapse of the I-35 Bridge in Minneapolis basically shows the

2

condition of infrastructures throughout the country. Thus, a severe infrastructure crisis exists and results in costly repairs and safety hazards. To alleviate this huge infrastructure deficiency; a novel, cost effective and environmental friendly strategies must be developed. Innovative materials can be used as a cost effective alternative to build new structure or replacement of these deteriorated structures which is often the only feasible solution.

1.2. BACKGROUND ON COMPOSITE MATERIALS

Advanced composites consisting of high strength fibers embedded in a resin matrix offer greatly reduced maintenance compared with steel and concrete and therefore offer whole life cost benefits. Implementation costs of fiber reinforced polymer materials, which is the only parameter used by clients in decision making, are higher than concrete and steel. But it is the paramount selection when the cost is calculated for the entire service life. Consequently, design methods have to be very sophisticated to avoid conservatism and material wastage and forms of structure must be optimized in terms of minimum material content.

The alternatives of replacement of existing structures have been proposed by researchers and there are numerous practical examples of those techniques (Hollaway and Leeming 1999). One of the most promising techniques is the application of fiber reinforced polymer (FRP) application which is comprised of unidirectional fibers embedded in a polymer resin and due to their very good properties like their tailoring properties, high weight to strength ratio, corrosion resistance, visco-elastic response, durability (chemical and fatigue resistance), ease of application due to their light weight and good adhesion (Teng et al.2003; Kim et al., 2008a, 2008b). FRP materials are superior to other materials like conventional steel reinforcement. The fibers provide load-carrying capacity of the

composite and the resin binds the fibers so that stress transfer between the fibers is achieved. After introduced in the construction industry FRP materials have given a boom in retrofitting and rehabilitation works. Fiber reinforced polymer (FRP) is widely used for retrofitting applications because of its high modulus, strength, and excellent durability. FRP composites may be externally bonded to the tensile soffit of a concrete member to increase load-carrying capacity.

1.3. RESEARCH OBJECTIVE

This research work is classified into two phases. Chapter 3 will cover up the entire program for phase I. Details derivation of equations along with case study related to phase I is described in Appendix C. The primary objective of phase I was to examine the time-dependent behavior of pultruded GFRP beam under sustained intensities and cold temperature. To obtain the main objective the following was conducted.

- Both experimental work and analytical study were performed to demonstrate the combined long-term loading and cold temperature effect on pultruded GFRP beam. The type of failure, change in load carrying capacity and maximum deflection were graphically presented in chapter 3.

Phase II will be discussed in chapter 4 which includes an experimental investigation on the short and long-term performance of near surface mounted (NSM) carbon FRP (CFRP) beam. The primary objective of this research work was:

- To compare the short-term behavior when loaded under monotonic and cyclic loading condition.

- To examine the effect of using different bonding agent on the load-carrying capacity and failure mode.

4

- To study the time-dependent performance during application of sustained load.

- To demonstrate the residual capacity and failure pattern after removal of sustained load.

1.4. SCOPE

The work shown in this thesis consists of two phases. Phase I focuses on GFRP material used for new construction and phase II deals with CFRP material for rehabilitation purposes.

The scope of Phase I includes the behavior of pultruded Glass FRP (GFRP) beams subjected to sustained intensities and cold temperature. Chapter 3 presents an experimental work that was conducted to understand the long-term (2000 hours) behavior of pultruded GFRP beams subjected to cold temperature ($-30^{o}C$) when associated with various loading conditions (20%, 40% and 60% of static capacity). An analytical model was developed based on regression analysis and a creep model was developed to predict the experimental behavior of the beams. The developed empirical model was incorporated into a finite element analysis with user-subroutines to predict the experimental findings. The behavior of the beams subjected to long-term loads was compared with that of the short-term beams. A parametric study was conducted to find the effects of these parameters on structural performances.

The scope of Phase II includes an experimental investigation into the short and long-term behavior of reinforced concrete beams strengthened with near surface mounted (NSM) carbon FRP (CFRP) strips. Chapter 4 contains an experimental study to compare the strength and failure mode of NSM beams with different bonding agent subjected to

monotonic and cyclic loading conditions. Then the strengthened beams were brought under three level of sustained loading (25%, 50%, and 75% of the static capacity) for a period of about 4000 hours. The long-term loading period was selected as 4000 hours considering that most of the creep will occur during this period (Deskovic et al. 1995). The variation of strains was recorded everyday during the period of sustained intensities. Finally, the residual capacity of the long-term beams was compared with that of the short-term control beams.

1.5. OUTLINE OF THESIS

This thesis is divided into five chapters and the summary of composition, mechanical properties of different types of fiber reinforced polymers (FRPs) and their long-term characteristics under sustained loading are discussed in the relevant chapters.

Chapter 1 addresses the introduction including the problem statement, general background and provides research objectives and scope of this research.

Chapter 2 represents a thorough review of available literatures regarding history of FRP composites, pultrusion process, time-dependent behavior of FRP composites and effect of temperature.

Chapter 3 describes the long-term behavior of glass fiber reinforced polymer (GFRP) beam at low temperature. A detailed description of the beams, experimental setup for sustained load and cold temperature, and a test scheme including an instrumental description is given in this chapter. The analytical modeling section consists of the equations used to predicts failure criteria and creep properties. The finite element modeling part includes sample details, element types, materials properties and failure criteria. This

chapter also contains the comparison of test results of the experimental and theoretical approach. Finally, a parametric study is performed.

Chapter 4 illustrates an experimental investigation into the short and long-term performance of reinforced concrete beams strengthened with near-surface mounted (NSM) carbon FRP (CFRP) strips subjected to sustained loads. The experimental program consists of beam details, sustained load and test scheme. A wide-ranging description of materials properties, sample preparation, test setup, instrumentation is given in this experimental program. This chapter also gives a brief comparison of test results which includes short and long-term behavior of NSM beam, adhesive test results and failure modes. Finally, the research findings are pointed out in the summery and conclusion section.

Chapter 5 represents conclusions from test results and provides selected observations and general comments on the recommendations for future work in this area. Though this thesis covers the time depended behavior of FRP composites, more research should be conducted to provide overall guideline for this materials. Very limited information is currently available regarding the effect of other factor such as cyclic loading and low temperature on FRP composites. Some future recommendations will be provided at end of this chapter.

Appendix A presents ASCE 2009 infrastructure progress report that shows the current infrastructure condition in the United States.

Appendix B includes recommended creep parameters for composite materials by ASCE structural plastic design manual (SPDM).

Appendix C contains derivation of equations used for analytical calculation, case study and detail database corresponding to Chapter 3.

Appendix D illustrates additional graphical information related to Chapter 4.

1.6. REFERENCES

ASCE. 2009. Report card for America's infrastructure, American Society of Civil Engineers, Reston, VA.

Deficient Bridge Report.2008.Federal Highway Administration.

Enright, M.P. and Frangopol, D.M. 2000. Survey and Evaluation of Damaged Concrete Bridges, Journal of Bridge Engineering, ASCE, 5(1), 31-38.

Kim, Y.J., Longworth, J., Wight, R.G., and Green, M.F. 2008(a). Flexure of two-way slabs strengthened with prestressed or non-prestressed CFRP sheets, Journal of Composites for Construction, 12(4), 366-374.

Kim, Y.J. and Heffernan, P.J. 2008(b). Fatigue behavior of structures strengthened with fiber reinforced polymers: state-of-the-art, Journal of Composites for Construction, 12(3), 246-256.

L C Hollaway and M B Leeming. 1999. Strengthening of Reinforced Concrete Structures – using externally-bonded FRP composites in structural and civil engineering, Woodhead Publishing, Abington Hall, Abington, Cambridge CB1 6AH UK. ISBN 85573 3781

Nikola Deskovic, Urs Meier, and Thanasis C. Triantafillou. 1995. Innovative Design of FRP Combined With Concrete: Long-Term Behavior. Journal of Structural Engineering, Vol.121, No.7. ©ASCE. ISSN 07339445/95/0007-1079-IOR9.Paper No. 6523.

Shahrooz, B.M., Tunc., G., Deason, J. T. 2002, RC/Composite Wall-Steel Frame Hybrid Buildings: Connections and System Behavior, Report No. UC-CII 02/01, Cincinnati Infrastructure Institute.

Teng, J.G, Chen, J.F., Smith, S.T., and Lam, L. 2003. Behavior and strength of FRP-strengthened RC structures: a state-of-the-art review, Structures and Buildings, ICE, 156(1), 51-62.

Wikipedia. 2009. List of bridge failures, www.en.wikipedia.org/wiki/List of_bridge_failures.

CHAPTER 2. LITERATURE REVIEW

2.1. GENERAL

This chapter represents the literature review on Fiber reinforced polymer (FRP) products and the effect of sustained load and temperature on their performances. FRP composites have several emerging application in civil infrastructure. These materials have been used for many decades and several excellent published literatures are available that cover the manufacturing, mechanics and design of fiber composite materials. However this literature review will be limited to pultruded glass fiber reinforced polymer (GFRP) beam and near surface mounted (NSM) fiber reinforced polymer (FRP) reinforcement for increasing the capacity of reinforced concrete structure. The objective of this chapter is to provide a state-of-the art review of the current progress of relevant research and information related to the aim of this research work. To provide a better understanding of the objective of this extensive research work, the relevant research and information regarding the performance of FRPs under sustained loading, cold temperature intensities and combination of them will be reviewed separately in the relevant chapters.

2.2. FRP FOR STRUCTURAL APPLICATION

Since the preceding decade there has been intensive escalation in the use of fiber reinforced polymer (FRP) composite materials as construction materials. FRP composites are very proficient for the appliance in civil infrastructure because of their high strength-to-weight and stiffness-to-weight ratios, corrosion resistance, short and long-term structural characteristic. Their application is mainly imperative in the renewal of constructed facilities infrastructure such as buildings, bridges, pipelines, etc. In recent times, their use has

improved in the rehabilitation of concrete structures, primarily due to their pliable performance characteristics, simplicity in applications and less life cycle expenses. The promising field of renewal engineering may preeminently illustrate the function of FRP composites in civil engineering. The renewal of the structural inventory, which is illustrated in Fig. 2.1, can be classified into (1) rehabilitation, including the applications towards repair, strengthening and retrofit of structures; and (2) new construction with all FRP solutions or new composite FRP concrete systems.
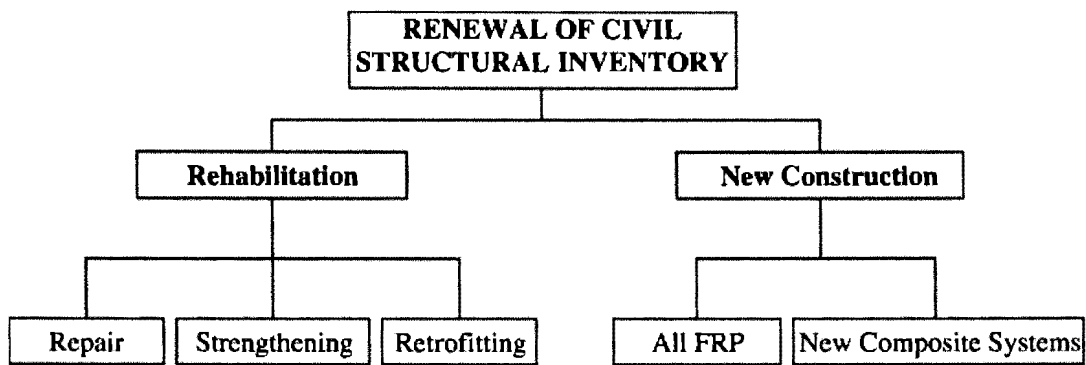
Fig. 2.1. Use of fiber reinforced polymer composites in civil engineering

Now, at the twenty-first century, the structural engineering society is about to cross a phase in which structural design with FRP composites is poised to become as practice as structural design with classical structural materials such as masonry, wood, steel, and concrete. In much the similar approach that a structural engineer has an operational understanding of the composition of structural materials such as steel, concrete, and wood and how they are prepared into products for structural applications, an analogous operational understanding of FRP composite materials is desirable by the structural

engineer. This cover up having a qualitative understanding of the constituent or raw materials and the processing schemes used to produce the parts and how these affect the eventual mechanical and physical properties of the FRP component. The intent of this chapter is to provide the structural engineer sufficient background about the prospective advancement in research and scope of FRP materials.

2.2.1. History of FRP Composites

FRP composites have been used insufficiently in structural engineering for almost 50 years for both new construction and rehabilitation of existing structures. After the Second World War, expansion in the construction industry led to a immense work load and much of the work was procured by the state with escalating bureaucracy in standards and specifications and little research and development. Composites have evolved since the 1950s, initially with impermanent structures and enduring with restoration of historic buildings and structural applications. The earliest experiment of FRP materials as reinforcement into reinforced concrete structures were sometime in the mid of 1950s (ACMA MDA 2006). The world's first road bridge using composite material is at Dusseldorf, Germany where in 1986, the 16m wide 47m span bridge used pre-stressed glass fiber/polyester resin pultruded rods. In 1991, strengthening of bridge girder using FRP composites first took place in Switzerland (ACMA MDA 2006). Then pedestrian bridge made of composite was built in 1992 at Aberfeldy, Scotland. In the United States, the first FRP-reinforced concrete bridge deck was installed at McKinleyville, West Virginia, in 1996 afterward the first all composite vehicular bridge deck in Russell, Kansas. Several composite pedestrian bridges have been established in U.S. state and national parks

11

in distant places not accessible by weighty construction equipment, or for spanning over roadways and railways (ACMA MDA 2006).

The up to date of the early work in the field of FRP composites for reinforcing and retrofitting of concrete structures in the United States, Japan, Canada, and Europe from 1980 to 1990 could be obtain from the collections of papers and reports edited by Nanni (1993b). A set journal associated with fiber reinforced polymers (FRPs) also reported by Iyer and Sen (1991). In 1993, a sequence of international conferences committed to FRP reinforcement of concrete structures was instigated (Bank 2006). These conferences have been held in different locations like Vancouver (1993), Ghent (1995), Sapporo (1997), Baltimore (1999), Cambridge (2001), Singapore (2003), Kansas City (2005), and Patras (2007). International research importance in the use of FRP in concrete improved considerably throughout this time. Since the early 1980s, Collections of papers on the use of FRP profile sections in structures have been published by the American Society of Civil Engineers (ASCE) and in proceedings of the ASCE Materials Congresses. A conversation was held at the Royal Society (1987) where a number of issues were made regarding the progress of materials throughout the ages. In 1994, the Latham report was published and regarded the construction industry as low technology, low skill and labor intensive compare with most other industries. The Journal of Composites for Construction, which nowadays is the prime international archive for reporting on research and progress in the field of FRP materials for the AEC industry, also founded by the American Society of Civil Engineers (ASCE) in 1997. In 2003, the International Institute for FRP in Construction (IIFC) was established in Hong Kong. Up to now, thousands of research program and structural engineering projects using FRP materials have been reported worldwide. Evaluation on the

advancement in this sector from 1990 to 2000 could be obtained in ACI (1996), Hollaway and Head (2001), Teng et al. (2001), Bakis et al. (2002), Hollaway (2003), Van Den Einde et al. (2003), and Tajlsten (2004).

In recent times, US Government along with private industries are making large investments in the high performance construction materials and systems. These construction materials consist of polymer composites and systems include innovative methods of construction. European government's initiatives have been slower than US but UK Government has commenced two programs with similar objectives to those in the USA, under the control of the EPSRC; these are the 'Innovative Manufacturing Initiative 1994' and the 'Materials for Better Construction Programme 1994.

2.2.2. Pultrution

Pultrusion is an automated manufacturing molding process for producing continuous lengths of FRP structural shapes. It is a cost-effective method of producing high-quality constant-cross-section of FRP profile. Its raw materials consist of a liquid resin mixture and reinforcing fibers. In this process, dry reinforcing fibers are pulled through a heated steel forming die using a continuous pulling device. The reinforcing fibers are in continuous forms such as rolls of fiberglass materials. As the reinforcements embedded in the resin mixture and pulled through the die, the gelation of the resin is initiated by the heat from the die and a rigid, cured profile is formed that corresponds to the shape of the die. The fundamental pultrusion process is depicted in the Fig. 2.2.

The function of guide is to locate the fiber reinforcement properly inside the composite. The position reinforcements for continuous supply into the guides ensure by creels. The impregnator contains solution of resin, fillers, pigment, catalyst and other

13

additives. Its interior is designed carefully to optimize the wet-out of the reinforcements. The reinforcement from guides saturates with the solution and organizes inside the resin bath. The performer squeezes away the excess resin and makes a perfect cross section before entering the die. The die provides both heating and curing to produce continuous rigid shape. The cooling is necessary to prevent the cracking and deformation in the profile. Then the cured profile is pulled to the saw for cutting to length.
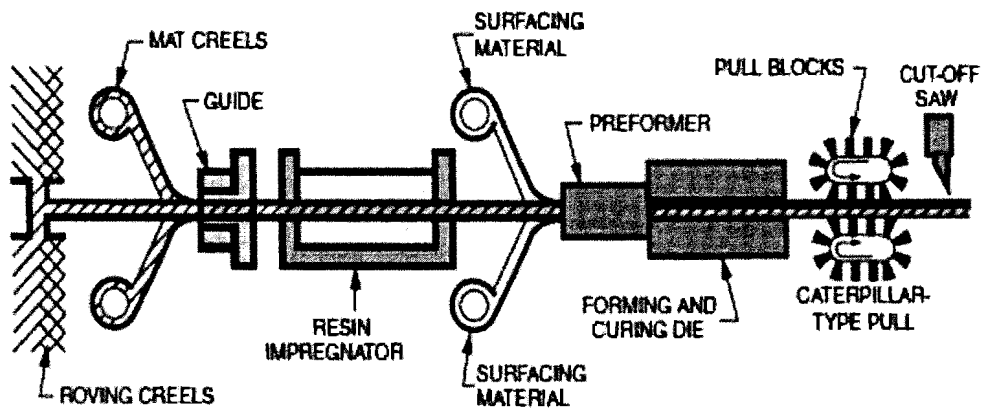
Fig. 2.2. Pultrusion (Strongwell design guideline)

Pultrusion process was developed in the 1950s in the United States to produce small profiles primarily for industrial applications, but the technique was always seen as being used to develop FRP alternative of conventional beams and columns for structural applications. Several pultrution industries were producing pultruded structural profiles from late 1960s. During this time, a commercial pultruded building system company named Composites Technology, Inc. (CTI) was founded by Andrew Green in Texas (Smallowitz 1985). They designed and constructed Electromagnetic Interference (EMI) laboratories for Apple computers. A single story building frame made of FRP profiles was

constructed for Electromagnetic Interference (EMI) test laboratories. The advantage of using FRP profile was electromagnetic transparency of FRP materials. Another FRP pultruded profile based structure constructed by Morrison Molded Fiberglass Company (MMFG, now Strongwell) for IBM in 1980s. In 1999, a Switzerland based company Fiberline Composites constructed a multistory framed building called the Eyecatcher for the Swissbau Fair as a demonstration of the potential for FRP profile shapes (Keller 1999).

In 1971, the structural research council (SPRC) was founded by the American Society of Civil Engineers (ASCE). The Structural Plastics Design Manual (SPDM) was developed for the design of structural plastics(McCormick 1988) which was originally published in 1979 as an FHWA report and afterward by the ASCE in 1984 (ASCE, 1984). Another design manual (Eurocomp 1996) developed in Europe for design of structures using advanced polymer composites. European Union also reported their first standard specification for pultruded profiles in 2002 (CEN 2002a). In addition with these manuals, allowable stress design (ASD) and load and resistance factor design (LRFD) and European limits states design (LSD) also applicable for design of FRP profiles. Creative Pultrusions also developed a design manual in late 1970s and updated versions of these manuals are available from these private industries. The manuals mentioned above do not include the optimized connection details for FRP profiles. Currently designers follow detailing similar to steel. More simple and effective connection system yet to be developed for commercial pultruded profiles.

FRP profiles were mostly used for bridge constructions and their applications initiated sometime in 1970s. Due to constant exposure on the environment, bridge structures are highly susceptible to corrosion effect. On the other hand installation of

lightweight member in bridge structure reduces the overall cost of a project. FRP profiles exhibits both noncorrosive and lightweight properties which is appropriate for bridge structures. FRP shapes generally used for bridge decking panels and superstructure members. However, in recent times FRP shapes also used in foundation piles. Pedestrian bridge with FRP truss member and deck panels designed and constructed with a span length varying from 9m to 27m. In 1990s, several bridge structures became deteriorated and innovative materials needed to develop for renovation of these structures. FRP profiles come as an alternative to replace existing bridge deck and girders. The long-term durability and lightweight were key benefit for using these materials. Private industries like Creative Pultrusions, Martin Marietta Composites, Atlantic Research Corp., Hardcore Composites commercially developed FRP deck during this time (Bakis et al. 2002). But due to connection design difficulties and high cost of glass FRP decks compared with conventional concrete decks the commercialization of FRP products were not extended up to a satisfactory level.

The use of carbon FRP cables for bridges was first suggested in the early 1980s for Materials Testing and Research (EMPA) in Dubendorf, Switzerland (Meier 1986). In 1992, Maunsell Structural Plastics designed and constructed a 131m long cable-stayed bridge in Aberfeldy, Scotland (Burgoyne and Head 1993; Cadei and Stratford 2002). They use Advanced Composite Construction System (ACCS) for designing the FRP plank system and fiber rope (Parafil) for the cable stays. In 1997, a 40.3-m cable-stayed pedestrian bridge was constructed over a railway line using FRP profiles in Kolding, Denmark (Braestrup 1999). At about this time, two carbon FRP cables consisting of 241.5mm diameter carbon-epoxy FRP rods were used in the Storchen cable-stayed bridge in

16

Winterthur, Switzerland. The largest size of unit that has been manufactured by the pultrusion technique to date is a double-webbed hybrid beam (36 in. high by 18 in. wide) designed by Strongwell in 2001 (Bristol, Va. USA). Carbon fiber cables were also used in the Laroin footbridge constructed in France in 2002.

2.2.3. Fiber Reinforced Polymer (FRP)

Fiber reinforced polymer (FRP) composites consist of a polymer resin matrix and reinforcing fibers. The strength, stiffness and durability of FRP mainly govern by the type and orientation of fibers within the composites. The desired structural characteristics and shapes obtain by controlling the placement and orientation of resulting fabrics. The fiber types that are typically used in the construction industry are carbon, glass and aramid. These common fibers used for the civil infrastructures are shown in Fig. 2.3, Fig. 2.4 & Fig. 2.5.

Carbon fibers are the stiffest, most durable, and most expensive fibers. Carbon is also quite resistant to most environmental conditions and can withstand high sustained and fatigue loading conditions. Glass fibers have lower strengths, stiffness and durability but at a reduced cost. The durability of glass fibers decreases due to most environments, especially hot/wet or highly alkaline environments. Glass is also susceptible to visco-elastic response which is eventual failure of the material under sustained loads higher than a fraction of the instantaneous ultimate load. CFRP materials have higher strength than GFRP materials. But GFRP composites are cheaper than CFRP composites. So we have to choose the optimum one based on strength required and cost analysis. Aramid fibers are less familiar in the construction industry. These fibers have similar characteristics between

those of glass and carbon but with improved durability and excellent impact resistance. Because of the impact resistance properties aramid fibers used in bulletproof jackets.

The resin binds the reinforcing fiber together and this resin bond aids in developing stiffness. It influences moisture stability, corrosion resistance, flame retardance, and maximum operating temperature of the composite. It is also responsible for certain failure characteristics including toughness and fatigue resistance. Two types of resin used in FRP materials such as thermosetting and thermoplastic resins. Thermosetting resins largely utilized by the construction industry. These resins start as a low viscosity, flowable material that cures to a final solid form. Epoxy and vinyl ester are the most commonly used thermosetting resins because of durability and adhesion properties. Most thermosetting resins are sensitive to heat and ultra-violet light exposure.

(a)   (b)

Fig. 2.3. Carbon-fiber reinforced polymer: (a) bar and strip; (b) woven fabrics (Focus Tech Ltd. 2010)

(a)   (b)
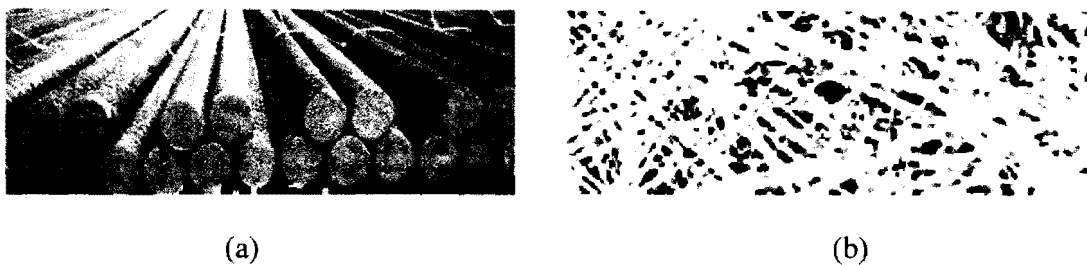
Fig. 2.4. Glass-fiber reinforced polymer: (a) bar; (b) woven fabrics (Focus Tech Ltd. 2010)

<div align="center">(a)   (b)</div>

Fig. 2.5. Aramid-fiber reinforced polymer: (a) rope; (b) woven fabrics (Focus Tech Ltd. 2010)

2.2.4. Rehabilitation

At the end of twentieth century, the most important challenges for the civil engineer were to repair and strengthening of deteriorated, damaged and substandard infrastructure. In many countries the rehabilitation of existing structures is fast growing especially in developed countries which completed most of their infrastructure in the first half of the last century. Many of the structures which were constructed after the World War II had little attention paid to durability issues. During this period, USA and Japan had inadequate understanding of seismic design and all of their infrastructures were not designed considering seismic criteria. These structures are now in need of urgent repair and retrofit. In the US infrastructure upgrading of structures has been estimated as $20 trillion (NSF 1993). For the seven year period between 1990 and 1996, 17% of the Federal-aid highway funds were spent for rehabilitation and replacement of existing bridges whereas only 4.5% was spent for construction of new bridges.

The rehabilitation techniques or FRP application can be primarily classified into active and passive where active means pre-stressed FRP materials are bonded and passive is just applying the strengthening materials without any pre-stressing. In a broad overview of the techniques it can be categorized as externally bonded and near surface mounted

<div align="center">19</div>

bonded one, to give a very brief history of post tensioning in reinforced concrete it can be documented that the post tensioning system either bonded or unbounded is being used since 1950's, which provide active reinforcement, using the same technique active FRP application is becoming popular for optimal use of high material properties of FRP. Similar to steel post tensioning where the existing beam/girder can deflect up, that is why this is considered as active method (EI-Hacha et. al 2004b; Millar et al. 2004; Nordin and Taljesten 2006; Badawi and Soudki 2006). Though the active or pre-stressing technique can be effective it can create secondary forces in indeterminate frames which is one of the toughest things in post tensioned concrete also the pre-stressing/post-tensioning itself is complicated (Zureick and Kahn 2001), so the most straightforward technique is the passive externally bonded technique/ NSM technique.

In Europe, the NSM technique was used for strengthening of concrete structure in early 1950s. A bridge deck in Sweden was upgraded by inserting steel bar in grooves at its tension face and filling it with cement mortar (Asplund 1949). Installation of FRP reinforcement rather than steel has several benefits for instance excellent resistance to corrosion, the ease of application due to lightweight properties and the reduced groove size due to higher tensile strength. NSM technique provides larger bond surface, better anchorage capacity, higher resistance against peeling-off, less preparation work, reduced installation (Nanni 2003; Cruz and Barros 2002). The NSM technique is attractive for strengthening in the negative moment region and provides an enhanced protection against high temperatures, fire, freeze-thaw cycles, ultraviolet rays and vandalism. The investigations demonstrated also an improved ductility, preferable composite action and an ultimate load develop more independent from concrete surface tensile strength (Cruz and

Barros 2002;Kotynia 2005). The adhesive used in NSM transfers the stresses between the FRP reinforcement and concrete. The most commonly used adhesives are epoxy and cement based. Though the two component epoxy is preferable, cement based adhesive also provides some advantages such as less expensive, less hazardous, applicable in wet surfaces, withstand in elevated temperatures and compatibility with the concrete. The adhesives should be selected based on its tensile and shear strength. The tensile strength is especially important in case of round bars which induce high circumferential tensile stresses in the epoxy (Lorenzis et al. 2002). The shear strength is especially important when the bond is controlled by cohesive shear failure of the epoxy (Teng et al. 2006). Epoxy materials properties depend on the time and temperature and affect the long-term response of the NSM structural members (Borchert and Zilch 2005). Cement mortar exhibits some limitation during groove filling (Lorenzis et al. 2002) and cyclic loading is not recommended in case of cement based adhesive (Borchert and Zilch 2005).

2.3. TEMPERATURE EFFECTS

Structural materials for cold regions have not received much concentration from scientific and engineering communities in the past. A very limited number of researches have been conducted on the mechanical properties of FRP under cold temperature intensities. In recent times, U.S. Army has been paid attention on the low-temperature influence on tensile and flexural strength of FRP composite laminate at Cold Regions Research and Engineering Laboratory (Dutta and Lampo 1993). Due to high coefficient of thermal expansion of FRP materials the effect of temperature must be considered during structural design particularly when used in conjunction with conventional construction materials (Hollaway and Head 2001). The characteristic varies with the temperature range

and it is generally determined by the secant gradient of the thermal expansion curve between a reference temperature (generally room temperature) and the working temperature. The differences of thermal expansion between fiber and matrix due to freeze-thaw environment also reported by Green (2007) and Täljsten et al. (2007).A number of researchers (Dutta et al. 1995) address low temperature effects on fiber composite and discovered slight negative coefficient of thermal expansion for CFRP in the range of -0.5×10^{-6} to -0.1×10^{-6} /°C and relatively high positive coefficient of thermal expansion for the polymer matrices in the range of 45×10^{-6} to 120×10^{-6} /°C. Mufti et al. (1991) also reported that the coefficient of thermal expansion of epoxy resins, glass fibers and carbon fibers are in the range of 45 to 65 $\times 10^{-6}$/°C, 5 $\times 10^{-6}$/°C and -0.2 to 0.6 $\times 10^{-6}$/°C respectively. The mismatch in coefficient of thermal expansions between fibers and matrices causes internal stresses at the fiber-matrix interface and generates micro-cracking. Most recently, the fatigue durability of FRP bridge decks and FRP-concrete hybrid bridge deck prototype under two extreme temperature conditions (−30°C and 50°C) was investigated (Dutta et al. 2007). The fatigue response of the deck prototypes was interrelated with the baseline performance of a conventional reinforced-concrete deck. Raiche (1999) inspected the creep durability of FRP (CFRP and GFRP) composites under different environmental effects such as moisture, temperature and deicing salts. Elastic modulus of the FRP composites materials was almost constant before and after environmental exposure. CFRP products showed excellent material properties under harsh environmental to GFRP product, despite higher water absorption. Cyclic freeze thaw under both dry and wet conditions degrades the strength and stiffness of carbon and glass fiber materials (Rivera and Karbhari 2001). The mechanical behavior of a honeycomb fiber-

reinforced polymer (HFRP) structure, supplied by Kansas Structural Composites, Inc. (KSCI), under the combined loading and temperature has been reported in a previous paper (Ma et al. 2007b). The panel stiffness was increased due to decrease in temperature from 26 to 0°C yet the stiffness was not further increased when the temperature was getting colder. They also observed that the degradation in stiffness could not be recovered by raising the panel temperature back to the room temperature. They did not clarify the reasons of this degradation. Instead, it was hypothesized that very cold temperature exposure resulted in matrix hardening and matrix micro-cracking. For the wide variety of FRP composites available for civil applications, the scarcity of performance records in cold regions poses a major problem for designers. More important, bridge decks are subjected to repeated loading from moving vehicles. Such repeated loads cause the stress in the deck to vary cyclically millions of times during the service life of the bridge. Thus, it is very important to consider the cold temperature effect on the behavior of FRP composite.

2.4. SUSTAINED LOAD

The long-term mechanical characteristics of polymer materials includes elastic and viscous phase hence they are classified as visco-elastic materials. The level and rate of sustained intensities affects their long term carrying capacity. The creep characteristic of a polymer composite is also influenced by the direction of alignment, the type and the volume fraction of the fibers. The effect of creep on the reinforcing fibers is very small (Ceroni et al. 2006). However, creep causes the progressive changes in the internal balance of forces within the materials and load transfer at the fiber-matrix interface (Chevali et al. 2009, 2010). Due to constant stress at a certain temperature the strain varies with respect to time. There are several methods around the world to represent the creep data. The most

familiar approach is to produce a set of creep curves in which the strains are measured at constant stress levels and plotted as a function of time. BS 4618 provides an alternative method for cross-plotting from creep curves at constant times. This yields a family of stress-strain curves, each relevant to a particular time of loading. By plotting the log strain versus log time axis, creep parameters can be obtained and when plotted in this manner most polymeric materials approximate to a linear relation. The creep parameters are dependent upon the stress level applied to the material and are a measure of its creep rate. To provide specific creep characteristics for polymers composite materials is very difficult because of its fiber volume fraction, fiber array and methods of manufacture will affect the results. Small test duration may be applicable in case of accelerated testing and mathematical formulation can be derived for extrapolated periods but it is dangerous to extrapolate values greater than three times the length of the test duration. In such case, sophisticated approach should be used such as the time temperature superposition principle (Aklonis and MacKnight 1983). The time applied stress superposition principle (Cessna 1971) can also be used for polymers and polymer composite materials. Due to variation of strain during the sustained loading periods the deflection increases beyond the instantaneous value and it depends on loading type, materials composition and testing condition. The deformational behavior of an advanced polymer composites has been discussed in Hollaway (1993).

The behavior of concrete structural member also affected by the stresses due to shrinkage, creep or the change of thermal coefficients of the constituent materials. Creep analysis of a concrete body depends on various factors such as concrete strength, the composition of the concrete, water contents, the dimensions of the element (Macgregor J.

24

G. 1997). ACI 209R (1992) provides specific guideline to predict time depended behavior of concrete subjected to sustained loading. Several experiments had been performed on the instantaneous deflections of reinforced concrete beams externally bonded with FRP system by (Chajes et al. 1994 and Ross et al. 1999). Chami et al. (2009) tested beams strengthened with externally bonded CFRP sheets where they found that the long term effect of the FRP was not significant for deflection control, this may be due to the fact that the major creep strain typically occur in the compression side of the beam however the flexural strengthening and crack control behavior was achieved by the strengthening schemes.

2.5. CONCLUSION

The fiber reinforced polymer composites are most attractive materials for potential applications in civil infrastructure due to their tailor ability and performances. Application of FRP materials can improve the overall quality of civil infrastructure to a satisfactory level.

From the literature review, it could be said that the time-depended behaviour of FRP materials subjected to sustained intensities associated with cold temperature reduces the load carrying capacity and stiffness of the structural member. The epoxy adhesive is also susceptible to the long-term effect and it should be considered during structural design.

More research should be conducted in the area of FRP materials to provide proper guideline to the professionals and convenient application of FRP materials. Additional attention needs to be paid on the long-term properties of FRP materials and low temperature effects on them. A complete discussion on this topic is given in the subsequent chapters.

2.6. REFERENCES

American Concrete Institute (ACI 440). 2007. Report on fiber-reinforced polymer (FRP) reinforcement for concrete structures. ACI Committee 440.XR-07, American Concrete Institute, Farmington Hills, Michigan, USA, pp.100.

American Concrete Institute (ACI 209R). 1992. Prediction of creep, shrinkage, and temperature effects in concrete structures. Manual of concrete practice, ACI Committee 209R, Detroit.

ACMA MDA. 2006. American composites manufacturers association market development Alliance, Arlington, Virginia, USA.

Aklonis, J. and MacKnight, W. 1983, An Introduction to Polymer Visco-elasticity, John Wiley and Sons, Ch.3.

Asplund, S.O. 1949. Strengthening bridge slabs with grouted reinforcement, J. Am.Concr. Inst. 45, no.1, 397–406.

Badawi, M., and Soudki, K. A. 2006.Strengthening of RC Beams with Prestressed Near Surface Mounted CFRP Rods, Proceedings of the 3rd International Conference on FRP Composites in Civil Engineering, Miami, FL, USA.

Bakis, C.E., Bank, L.C., Brown, V.L., Cosenza, E., Davalos, J.F., Lesko, J.J., Machida, A., Rizkalla, S.H. and Triantaffillou, T. 2002. Fiber-reinforced polymer composites for construction: state-of-the-art review, Journal of Composites for Construction, ASCE, 6(2):73-87.

Bank, L.C. 2006.Composites for construction, John Wiley & Sons, Hoboken, NJ.

Borchert, K., Zilch, K. 2005. Time depending thermo mechanical bond behavior of epoxy bonded pre-stressed FRP-reinforcement.

Braestrup, M. 1999. Footbridge constructed from glassfibre- reinfroced profiles, Denmanrk. Structural Engineering International, IABSE, 9(4):265-258.

Burgoyne, C., and Head, P. R. 1993.Aberfeldybridge: an advanced textile reinforced footbridge, presented at the TechTextil Symposium, Frankfurt, Germany.

Cadei, J., and Stratford, T. 2002. The design, construction and in-service performance of the all-composite Aberfeldy footbridge, in Advanced Polymer Composites for Structural Applications in Construction, pp. 445–455. Thomas Telford, London

CEN 2002, Reinforced Plastic Composites: Specifications for PultrudedProfiles,Parts 1–3, EN 13706, Comite' Europe'en de Normalisation, Brussels, Belgium

Ceroni, F., Cosenza, E., Gaetano, M., and Pecce, M. 2006. Durability Issues of FRP Rebars in Reinforced Concrete Members, Cement and Concrete Composites, Vol. 28, No. 10, pp. 857-868.

Cessna, LC. 1971. Stress–time superposition for creep data for polypropylene and coupled glass reinforced polypropylene. PolymEng Sci.

Chami, G. A., Thériault, M., Neale, K.W. 2009. Creep behaviour of CFRP-strengthened reinforced concrete beams, Construction and Building Materials, Volume 23, Issue 4, Pages 1640-1652

Chajes, M. J., Thomson, T. A., Jr., Januszka, T. F., and Finch, W. W., Jr. 1994. Flexural strengthening of concrete beams using externally bonded composite materials. Constr. Build. Mater., 8(3), 191–201.

Chevali, V.S., Dean, D.R., Janowski, G.M. 2009. Flexural creep behavior of discontinuous thermoplastic composites: Non-linear viscoelastic modeling and time-temperature-stress superposition. Composites A40, 870–877

Chevali, V. S., Janowski, G. M. 2010. Flexural Creep of Long Fiber-Reinforced Thermoplastic Composites: Effect of Processing-Dependent Fiber variables on Creep Response Composites, Part A: Applied Science and Manufacturing.

Cruz, J.M.S, Barros, J.A.O. 2002. Bond behavior of carbon laminates strips into concrete by pullout-bending tests, Proceedings, Int. symposium on Bond in concrete-from research to standards, pp. 614–622.

De Lorenzis, L., Rizzo, A., La Tegola, A. 2002. Modified pull-out test for bond of near-surface mounted FRP rods in concrete, Composites: Part B Engineering 33, 589–603.

Dutta, P. K., and Lampo, R. G. 1993.Behavior of fiber-reinforced plastics as construction materials in extreme environments.Proc.,3rd Int. Offshore and Polar Engineering Conf., 339–344.

Dutta, P. K., and Hui, D. 1996.Low-temperature and freeze–thaw durability of thick composites.Composites, Part B, 27(3–4), 371–379.

Dutta, P. K., Lopez-Anido, R., and Kwon, S. K. 2007. Fatigue durability of FRP composite bridge decks at extreme temperatures. Int. J.Mater. Prod. Technol., 28(1/2), 198–216.

Eurocomp. 1996. Structural Design of Polymer Composites: EUROCOMP Design Code and Handbook, Clark, J. L. (ed.) E&FN Spon, London.

El-Hacha, R., Green, M. F., and Wight, R. G. 2004(b). Flexural Behaviour of Concrete Beams Strengthened with Prestressed Carbon Fibre Reinforced Polymer Sheets Subjected

to Sustained Loading and Low Temperature, Canadian Journal of Civil Engineering, V. 31, pp. 239-252

Focus Tech Ltd. 2010.http://pulwell.en.made-in-china.com/custom/xJQxmEnAMEhQ/Hot-Products-1.html

Green. 2007. FRP Repair of Concrete Structures: Performance in Cold Regions, *Int. J. of Mat. and Prod. Tech.,*28(1/2): 160-177

Hollaway, L. 1993. Polymer Composites for Civil and Structural Engineering,Chapman& Hall, New York.

Hollaway, L., and Head, P. R. 2001.Advanced polymer composites andpolymers in the civil infrastructure, Elsevier Science, Amsterdam, The Netherlands.

Hollaway, L.C. 2003, The evolution of and the way forward for advanced polymer composites in the civil infrastructure, Composites and Building Materials,vol. 17, pp. 365-378.

Iyer, S. L. and Sen, R. 1991.Advanced composite materials in civil engineering structures, Proc. Specialty Conf., Las Vegas, Jan. 31- Feb. 1, American Society of Civil Engineering, New York, NY.

Keller, T. 1999. Towards structural forms for composite fiber materials.Struct. Eng. Int. (IABSE, Zurich, Switzerland), 9(4), 297–300

Kotynia, R. 2005. Strain efficiency of near-surface mounted CFRP-strengthened reinforced concrete beams, Third international conference composites in construction, Lyon, 2005, pp. 35–42.

Ma, Z., Chaudhury, S., Millam, J., and Hulsey, J. L. 2007(a).Field test and 3D FE modeling of decked bulb-tee bridges.J. Bridge Eng., 12(3), 306–314.

Ma, Z., Choppali, U., and Li, L. 2007(b). Cycling tests of a fiber reinforced polymer honeycomb sandwich deck panel at very cold temperatures. Int. J. Mater. Prod. Technol., 28(1/2), 178–197.

Macgregor, J. G., 1997, Reinforced Concrete: Mechanics and design, Third Edition, Prentice Hall

McCormick, F. C. 1988. Advancing structural plastics into the future, Journal of Professional Issues in Engineering, Vol. 114, No. 3, pp. 335–343.

Meier, U. 1986. Proposal for a Carbon Fibre Reinforced Composite Bridge Across the Strait of Gibraltar at its Narrowest Site. Proceedings of the Institute of Mechanical Engineers, 201, 73-78

Millar, D., Scott, P., and Clenin, R. 2004. Bridge Strengthening with Prestressed CFRP Plate System, Proceedings of the second international conference on FRP composites in civil engineering, Adelaide, Australia, pp. 463-469.

Mufti, A., Erki, M. A. and Jaeger, L. 1991.Advanced composite materials with application to bridges,Canadian Society of Civil Engineers, Montreal

Nanni, A. 1993. Fiber-Reinforced-Plastic (FRP) Reinforcement for Concrete Structures: Properties and Applications, Developments in Civil Engineering, Vol. 42, Elsevier, Amsterdam, The Netherlands, pp. 450

Nanni, A.2003. North American design guidelines for concrete reinforcement and strengthening using FRP: principles, applications and unresolved issues, Construction and Building Materials 17, 439–446.

Nordin, H., and Taljsten, B. 2006. Concrete beams strengthened with prestressed near surface mounted CFRP, Journal of Composites for Construction, V. 10, No. 1, pp. 60-68.

Rivera, J., and Karbhari, V. M. 2001.Characterization of sub-zero response of vinylester FRP in civil infrastructure renewal.Proc., 11th Int. Offshore and Polar Engineering Conf., 124–30.

Ross, C. A., Jerome, D. M., Tedesco, J. W., and Hughes, M. L. 1999. Strengthening of reinforced concrete beams with externally bonded composite laminates. ACI Struct. J., 96(2), 212–220.

Raiche, A. 1999. Durability of Composite Materials used as external reinforcement for RC beams, Annual Conference of the American Society for Civil Engineering, Regina, Saskatchewan, Canada, pp. 155-164

Smallowitz, H. 1985. Reshaping the future of plastic buildings.CivilEng. (N.Y.), 55, 38–41.

Teng, J. G., Chen, J. F., Smith, S. T. & Lam, L. 2002. FRP Strengthened RC Structures, Chichester, John Wiley & Sons.

Teng, J.G., de Lorenzis, L., Wang, B., Li R, Wong, T.N., Lam, L. 2006.Debonding failures of RC beams strengthened with near surface mounted CFRP Strips, Journal of composites for construction 10, no. 2, 92–105, DOI 10.1061/(ASCE)1090-0268(2006)10:2(92).

Tajlsten, B. 2004.FRP Strengthening of Existing Concrete Structures – Design Guidelines.Lulea University Printing Office, Lulea, Sweden.

Täljsten, B., Bergström, M., Enochsson, O. &Elfgren, L. 2007.CFRP strengthening of the Örnsköldsvikbridge.Sustainable bridges : assessment for future traffic demands and longer lives, DolnoslaskieWydawnictwoEdukacyjne, 355-364

Van Den Einde, L.; Zhao L.; Seible, F. 2003. Use of FRP composites in civil structural applications, Construction and Building Materials 17(6–7): 389–403.

Zureick, A., and Kahn, L. 2001. Rehabilitation of Reinforced Concrete Structures Using Fiber-Reinforced Polymer Composites, ASM Handbook, ASM International, V. 21, pp. 906-913.

CHAPTER 3. TIME-DEPENDENT AND RESIDUAL BEHAVIOR OF PULTRUDED GFRP BEAMS SUBJECTED TO SUSTAINED INTENSITIES AND COLD TEMPERATURE

3.1. SYNOPSIS

This chapter[1] presents the time-dependent response and residual behavior of pultruded glass fiber reinforced polymer (GFRP) beams. A total of nine beams are tested in four-point bending, including one control beam without external load and the remaining beams are subjected to three levels of sustained intensities (20%, 40%, and 60% of the static capacity) at room (25°C) and cold (-30°C) temperatures for 2,000 hours. Time-dependent material parameters are obtained from the test. Analytical approaches are used to predict the behavior of test beams, based on mechanics-based failure criteria and Findley's creep theory. Three-dimensional finite element models are also developed, based on the experimentally obtained material parameters. The GFRP beams demonstrate time-dependent material degradation due to the sustained load. The effect of cold temperature alters the load-carrying capacity and creep response of the beams. The brittle behavior of the GFRP is accelerated when the beams are exposed to sustained intensities and cold temperature. The contribution of shear deformation to the deflection of the beams increases with sustained load. Although the proposed modeling approaches agree with the experiment, further development is recommended to account for micro-level material deterioration characteristics.

---

[1] This chapter has been submitted to the Journal of Composites for Construction, ASCE for possible publication

31

3.2. INTRODUCTION

The need for sustainable materials is emerging in the infrastructure community to address the considerable maintenance expense of structural members made of conventional construction materials. For instance, corrosion is a major factor influencing the long-term performance of steel beams. Glass fiber reinforced polymer (GFRP) composites may be a strong alternative to such materials. GFRP structural shapes are manufactured by a continuous process, called *pultrusion*: high-strength fibers are pulled through a resin container and heated to polymerize the resin to form a hardened shape (Zureick 1998). Like structural steel members, pultruded GFRP sections can be open or closed. The benefits of GFRP applications encompass high strength-to-density ratios, resistance to environment, enhanced long-term durability, low labor cost, accelerated construction time, lower transportation cost, and reduced maintenance expense (Zureick 1998; Nordin et al. 2010). Pultruded GFRP members are broadly used for civil engineering applications, including buildings, bridges, transmission towers, and guardrails (Bank 2006).

Fundamental behavior and structural response of pultruded GFRP composites have been extensively studied. Bank (1987) addressed a method to estimate the flexural and shear moduli of pultruded GFRP beams. It was found that the contribution of shear deformation to beam deflection was not negligible for GFRP materials because of their anisotropic material properties. Neto and Rovere (2007) confirmed this conclusion using experimental and numerical approaches. Bank and Mosallam (1992) studied the long-term behavior of a frame structure fabricated with pultruded GFRP shapes. In addition to experimental investigations, a model was developed using Findley's creep theory to predict the creep response of GFRP. It was recommended that time-dependent material constitutive

characteristics be explicitly included in the design and analysis of pultruded GFRP shapes. Zureick (1998) performed an extensive review concerning pultruded GFRP for structural applications, including material behavior and design. The review highlighted the importance of experimental observations and the need for design criteria to widely disseminate the promising material for structural applications. Keller et al. (2007) tested a truss bridge fabricated with pultruded GFRP shapes. The bridge was exposed to pedestrian and environmental loads for eight years and was taken down for a laboratory investigation. According to test results, GFRP shapes did not show noticeable stiffness degradation; however, inappropriate detailing of the structural system affected the long-term performance of GFRP. Bai and Keller (2009) studied the time-dependent behavior of GFRP composites in fire with emphasis on thermo-physical and thermo-mechanical properties. Thermal conductivity predicted by a numerical model was compared with measured experimental data.

Prefabricated GFRP composites are particularly useful for cold region applications, taking into account limited construction availability. Rivera and Karbhari (2001) examined the freeze-thaw behavior of GFRP composites. The plasticization and brittleness of GFRP were influenced by a combination of moisture-induced hydrolysis and thermal cracking. Dutta et al. (2007) performed an experimental investigation to evaluate the fatigue behavior of deck slabs fabricated with pultruded GFRP when exposed to a temperature of -30°C. Test results were compared with those of conventional reinforced concrete decks. The effect of temperature was noticeable, while that of fatigue cycles was insignificant. Nordin et al. (2010) examined the material characteristics of GFRP composites subjected to variable temperatures ranging from 24°C to -35°C. GFRP coupons were tested in uniaxial

and biaxial loading conditions, including elevated strain loads. Experimental results showed that cold temperature effects accelerated the deterioration of GFRP materials.

Although extensive research has been conducted in the area of pultruded GFRP composites as discussed above, there still exist insufficient understandings of the behavior of GFRP when it comes to cold region applications. In particular, very limited experimental data are available for the long-term behavior of GFRP shapes in such environments. Given that structural members on site are subjected to permanent loads, synergetic effects of sustained intensities and cold temperature exposure may influence the behavior of GFRP members situated in cold regions. This chapter presents an experimental investigation concerning the long-term performance of pultruded GFRP I-beams subjected to sustained loads associated with cold temperature (-30°C). Predictive responses are discussed using an analytical creep model and a three-dimensional finite element (FE) analysis. Design considerations are addressed for practical applications of pultruded GFRP shapes in cold regions.

3.3. RESEARCH SIGNIFICANCE

Serviceability limit state frequently governs the design of GFRP structural shapes, rather than strength limit state, because of their low modulus (Roberts and Masri 2003). Long-term deflection of such members is, therefore, an important consideration from a practical point of view. Time-dependent response of GFRP composites under external load is of interest to understand their long-term performance, provided that such materials exhibit viscoelastic characteristics (Zureick 1998). Very limited information is currently available on the behavior of GFRP shapes subjected to sustained intensities in cold region

environment. The experimental research presented here will address these critical research needs to improve the current knowledge concerning design and practice.

3.4. EXPERIMENTAL PROGRAM

3.4.1. Beam Details

A total of nine GFRP beams were tested, one of which served as a control beam and the remaining beams were subjected to various sustained intensities at room (25°C) and cold (-30°C) temperatures, as shown in Table 3.1. The pultruded I-shape beam used here consists of glass fibers embedded in a vinylester resin matrix, including a fiber volume fraction ratio of 55% (Strongwell 2009). The GFRP shape includes fire-resisting additives to conform to the requirements of ASTM E84 (ASTM 2010a) and ASTM D635 (ASTM 2010b). The beam section had a nominal depth of 101.6 mm and a flange width of 50.8 mm with a thickness of 6.4 mm, as shown in Fig. 3.1. Selected material properties of the GFRP are summarized in Table 3.2. An ancillary test was conducted to confirm the longitudinal tensile modulus and corresponding strength provided by the manufacturer. Three dog-bone

Table 3.1. Beam details and test results

Beam	Temperature	Sustained load[a]	Load-carrying capacity					
			Experimental		FEA		Analytical	
			Load (kN)	Ratio (%)[b]	Load (kN)	Ratio (%)[b]	Load (kN)	Ratio (%)[b]
Control	25°C	0%	31.5	100.0	31.5	100.0	34.7	100.0
R60-1	25°C	60%	27.6	87.6	31.1	98.7	34.2	98.6
R60-2	25°C	60%	27.9	88.6	31.1	98.7	34.2	98.6
C20-1	-30°C	20%	29.5	93.7	31.5	100.0	34.9	100.6
C20-2	-30°C	20%	30.9	98.1	31.5	100.0	34.9	100.6
C40-1	-30°C	40%	27.0	85.7	30.6	97.1	33.5	96.5
C40-2	-30°C	40%	29.7	94.3	30.6	97.1	33.5	96.5
C60-1	-30°C	60%	24.0	76.2	28.8	91.4	31.9	91.9
C60-2	-30°C	60%	28.8	91.4	28.8	91.4	31.9	91.9

[a]: sustained for 2,000 hours
[b]: ratio between beam capacity/control capacity

Table 3.2. Materials properties of GFRP composite

Property	Value[a]
Longitudinal tensile strength (σ_t^L)	207 MPa
Longitudinal compressive strength (σ_c^L)	207 MPa
Transverse tensile strength (σ_t^T)	48.3 MPa
Transverse compressive strength (σ_c^T)	103 MPa
Longitudinal tensile modulus (E_t^L)	17.2 GPa
Longitudinal compressive modulus (E_c^L)	17.2 GPa
Transverse tensile modulus (E_t^T)	5.5 GPa
Transverse compressive modulus (E_c^T)	5.5 GPa
Major Poisson's ratio	0.33

[a]: manufacturer (Strongwell 2009)

coupons (15 mm wide × 200 mm long × 6.4 mm thick) were extracted from a GFRP beam and loaded in tension until failure occurred. Such a sampling method provides more reliable material properties when compared to a solid-bar coupon test (Deskovic et al. 1995). The tension test results agreed well with the manufacturer's properties with an average error of 3.3% in tensile strength, as shown in Fig. 3.2. Longitudinal properties have the main contribution to the flexural response. That's why coupon test was performed to verify manufacturer properties in this direction.
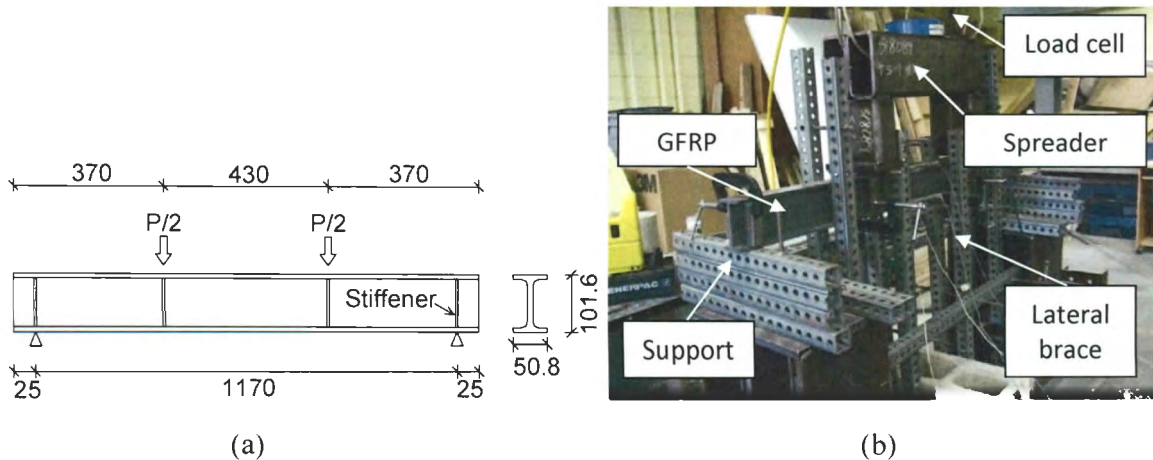
Fig. 3.1. Beam detail and test set-up: (a) GFRP beam (unit in mm); (b) load test
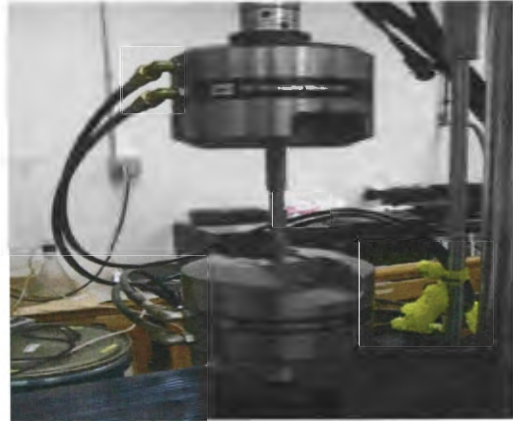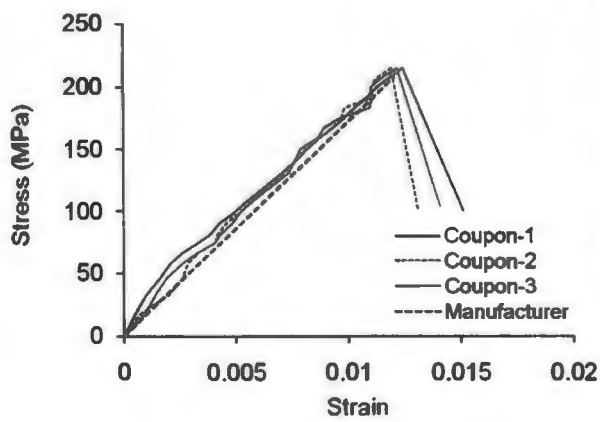
Fig. 3.2. Constitutive behavior of GFRP: (a) coupon test in tension; (b) stress-strain relationship

3.4.2. Sustained Load and Cold Temperature Exposure

A custom-made loading apparatus with a hydraulic jack was used to apply long-term load to the beams in four-point bending [Fig. 3.3(a)]. The levels of sustained load were 20%, 40%, and 60% of the load-carrying capacity (P_u) of the static control beam (Table 3.1). These intensities were assumed to represent typical service load levels. A strain gage was bonded to the tensile surface of the GFRP beams at midspan to monitor their response during a jacking operation. Once the target load level was achieved, the jacking load was transferred to the beams using a clamping system that consisted of hollow square steel sections (50 mm × 50 mm) with Φ9.5 mm threaded rods [Fig. 3.3(b)]. Lateral supports were added to prevent potential torsional buckling of the beams during a test period of 2,000 hours. The long-term simulation time was determined based on Bank and Mosallam (1992) indicating that the major creep of pultruded GFRP beams had occurred during the first 2,000 hours after loading. A pair of the beams loaded to $60\%P_u$ was exposed to room temperature for 2,000 hours (Beams R60-1 and -2), whereas other beams

37

were situated inside an environmental chamber for cold temperature exposure at -30°C [Fig. 3.3(c)] for the same period of time. The chamber was equipped with a digital temperature adjustment function that provided real-time temperature data. The strain of the beams at room temperature was consistently monitored until the long-term simulation was completed; however, the strain gages of the beams in the environmental chamber were disconnected from the data acquisition system because they were not waterproof.

<div align="center">(a)   (b)   (c)</div>
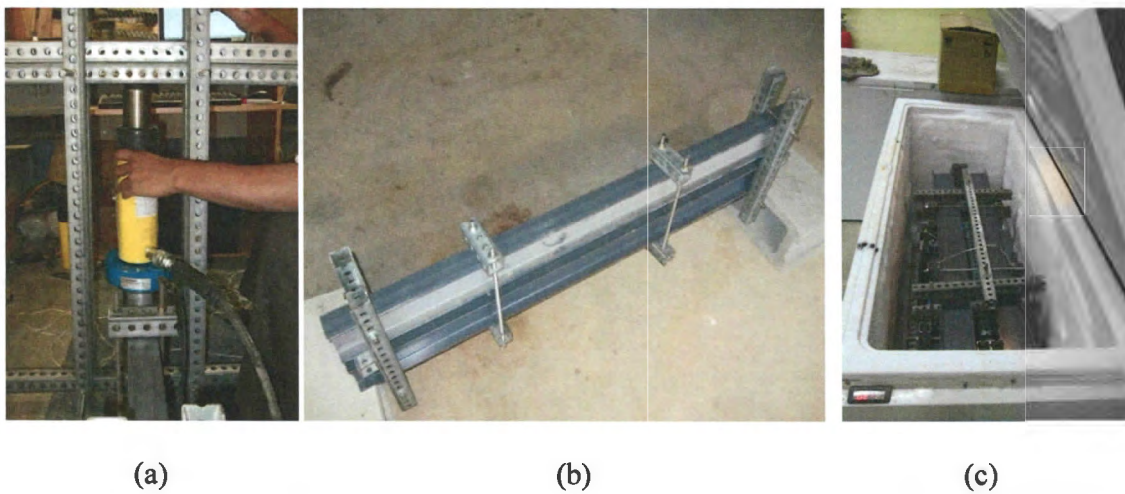
Fig. 3.3. Long-term load application: (a) jacking operation; (b) transferred sustained load; (c) cold temperature exposure at -30°C

3.4.3. Test Schemes

The control beam without long-term load was loaded in four-point bending with a simple span of 1,170 mm, as shown in Fig. 3.1. The load was statically applied until failure occurred. Upon completion of the long-term process (Fig. 3.3), all beams that had been exposed to -30°C were loaded in a same manner (i.e., four-point bending) to examine their residual performance such as load-carrying capacity and flexural modulus. Great care was exercised to preclude lateral torsional buckling during the load test (Fig. 3.1), taking into account the slender geometry of the GFRP beam (details will be discussed in the *Failure*

Criteria section). A linear potentiometer (LP) was positioned at midspan of each beam to measure deflection. Two displacement-type strain transducers (so called *PI gage*) having a gage length of 100 mm were installed to record tension and compression strains at the upper and lower flanges.

3.5. ANALYTICAL MODELING

3.5.1. Failure Criteria

To predict the load-carrying capacity of the GFRP beams, failure criteria were established. Several failure modes were accounted for to address the complex failure mechanism of the thin-walled beams such as buckling and shear fracture. For the present study, mechanics-based equations available in Bank (2006) were adopted as summarized below. Material characteristics of GFRP are represented by orthotropic properties (Table 3.2). The critical stress for lateral torsional buckling (σ_{cr}^{LTB}) may be obtained using Eq. 3.1:

$$\sigma_{cr}^{LTB} = \frac{C_b}{S_x} \sqrt{\frac{\pi^2 E_L I_y G_{LT} J}{\left(k_f L_b\right)^2} + \frac{\pi^4 E_L^2 I_y C_w}{\left(k_f L_b\right)^2 \left(k_w L_b\right)^2}} \qquad (3.1)$$

where C_b is the moment coefficient ($C_b = 1.13$ for the simply-supported beam in uniform load); S_x is the section modulus about the strong axis; E_L, I_y, G_{LT}, and J are the longitudinal modulus, moment of inertia in the weak axis, longitudinal shear modulus, and polar moment of inertia, respectively; k_f and k_w are the end restrained coefficients ($k_f = k_w = 1.0$ for the simply-supported beam with lateral supports); and C_w is the warping coefficient of the section ($C_w = I_y d^2 / 4$ where d is the depth of the beam). The local buckling of a GFRP section may take place when the applied stress exceeds the following limits:

$$\sigma_{cr}^{flange} = \frac{1}{\left(b_f/2\right)^2 t_f}\left(7\sqrt{\frac{D_L D_T}{1+4.12\zeta}}+12D_s\right) \tag{3.2}$$

$$\sigma_{cr}^{web} = \frac{2\pi^2}{t_w d_w^2}\left(\sqrt{D_L D_T}+D_{LT}+2D_s\right) \tag{3.3}$$

where σ_{cr}^{flange} and σ_{cr}^{web} are the critical stresses for the flange and web buckling of the section; D_L, D_T, and D_{LT} are the plate flexural rigidities in the longitudinal (L) and transverse (T) directions ($D_L = E_L t^3/[12(1-v_L v_t)]$, $D_T = (E_T/E_L)D_L$, and $D_{LT} = v_T D_L$ in which t = plate thickness, E_T = elastic modulus perpendicular to the fiber direction, and v_L and v_T = Poisson's ratios in the longitudinal and transverse directions, respectively); D_s is the shear rigidity ($D_s = G_{LT} t^3/12$); ζ is a non-dimensional restrained coefficient ($\zeta = D_t/kLt$ in which k= rotational spring constant); t_w is the thickness of the web; and d_w is the depth of the web. The web shear failure of a section may be predicted using Eq. 3.4:

$$\tau_{cr}^{web} = \frac{4k_{LT}\sqrt[4]{D_L D_T^3}}{t_w d_w^2} \tag{3.4}$$

where τ_{cr}^{web} is the critical shear stress in the web and k_{LT} is the shear buckling coefficient (k_{LT} = 8.125+5.045 $[2D_s+D_{LT}/(D_L D_T)^{1/2}]$. Upon computing all failure criteria, the governing failure is determined based on the following assumption: a specific failure mode predominates over other failure modes of the beam when the calculated stress using fundamental elastic theory exceeds corresponding stress limit. The most critical failure

40

mode of the beam was lateral torsional buckling (to be discussed) due to the slender geometry [Fig. 3.1(a)]. Such a failure was, however, effectively precluded using heavy lateral bracing members [Fig. 3.1(b)].

3.5.2. Modeling of Creep Behavior and Long-term Properties

Findley's creep theory was adopted to predict the time-dependent behavior of GFRP. Although this theory has some limitations (Shao and Shanmugam 2004), it is still widely used in the research community (Bank and Mosallam 1992; Scott and Zureick 1998; Shao and Shanmugam 2004). The model consists of elastic and viscous strains as shown in Eq. 3.5 (Findley 1960):

$$\varepsilon = \varepsilon_i + m\left(\frac{t}{t_i}\right)^n \tag{3.5}$$

where ε is the time-dependent strain; ε_i is the instantaneous elastic strain; m and n are the material constants; and t_i and t are the initial and current times, respectively. The material constants m and n for GFRP composites may be available from creep tests with Eq. 3.6 (by taking the log of Eq. 3.5):

$$\log(\varepsilon - \varepsilon_i) = \log(m) + n\log\left(\frac{t}{t_i}\right) \tag{3.6}$$

The time-dependent viscoelastic modulus of GFRP (E_v) can then be derived from Eq. 3.5 with a condition of $m = \sigma/E_t$ where σ is the applied stress at time t and E_t is the

corresponding modulus:

$$E_v = \frac{E_i}{1 + \left(\dfrac{m}{\sigma} E_i\right) t^n}$$

(3.7)

where E_i is the initial elastic modulus of the GFRP. The residual modulus (E_r) of all test

beams (when mechanically loaded after exposure to -30°C for 2,000 hours) may be

obtained using elastic theory:

$$E_r = \frac{PaKAG\left(3L^2 - 4a^2\right)}{24I\left(2KAG\delta - Pa\right)}$$

(3.8)

where P is the applied load [Fig. 3.1(a)]; a and L are the shear- and loading-span lengths of

the GFRP beam in four-point bending, respectively; δ is the measured midspan deflection

of the beam; A and I are the cross-sectional area and moment of inertia, respectively; G is

the shear modulus; and K is the shear coefficient ($K = 0.413$ was obtained for the present

beams based on Bank 1987). It can be reasonably assumed that other orthogonal material

properties (Table 3.2) are scaled with the variation of the longitudinal modulus because

GFRP exhibits linear elastic characteristics up to failure. The analytical deflection of the

GFRP beam can be calculated using structural analysis equations, consisting of flexural and

shear components as discussed in Appendix C.

3.6. FINITE ELEMENT MODELING

A three-dimensional FE model was developed using the general-purpose software ANSYS to predict the behavior of the GFRP beams, as shown in Fig.3.4. GFRP was modeled using structural solid elements (SOLID45). This element consists of eight nodes with three translational degrees of freedom at each node. Orthotropic properties are required to represent material characteristics. Elastic shell elements (SHELL63) were used to model vertical stiffeners at loading points. The material properties of SHELL63 were assumed to be those of typical structural steel with an elastic modulus of 200 GPa and Poisson's ratio of 0.3. The stiffener geometry was simplified for modeling convenience in such a way that the hollow steel section (25 mm wide × 25 mm deep × 2.5 mm thick) was represented by an equivalent cross-sectional area of the shell element. The Tsai-Wu failure criterion was incorporated into the developed model to predict the failure of GFRP (Tsaiand Wu 1971). Such a failure prediction takes into consideration multi-axial stress states that can be compatible with the analytical failure criteria established in Eqs. 3.1 through 3.4. To preclude the potential warping of the thin flanges and web, the aspect ratio of the model was controlled (i.e., thickness to length ratio = 1 to 4). Boundary conditions were applied to represent a simply-supported condition by constraining necessary nodes near both ends of the beam. Loads were incrementally applied until the Tsai-Wu failure criterion was reached. A sensitivity analysis was conducted to determine the adequate mesh size of the model using the control beam, as shown in Fig. 3.4.
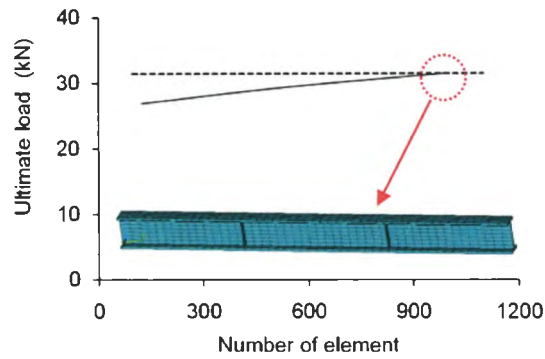
Fig. 3.4. Mesh sensitivity analysis using control beam

3.7. TEST RESULTS AND ANALYSIS

3.7.1. Creep Parameters and Residual Modulus

Fig.3.5. shows the measured time-dependent strains of the test beams at midspan during jacking and transfer of the sustained loads. The strain response tended to be stable in 15 minutes after load-transfer from the jacking apparatus to the beams. A relatively significant transfer loss was observed for the beam loaded at $60\%P_u$. The effective strains of the beams after 30 minutes of the transfer were 16.0%, 29.6%, and 41.6% of the tensile rupture strain in the longitudinal direction of the GFRP (ε_L^{fu}) for the beams with sustained intensities of 20%, 40%, and $60\%P_u$, respectively, as shown in Fig. 3.5. The time-dependent creep parameters m and n (Eq. 3.6) of the long-term control beam (Beam R60-1) were determined using the strains measured for 2,000 hours (Fig. 3.6). The initial time (t_i) was assumed to be unity (Bank and Mosallam 1992) and the initial elastic strain (ε_i) was calculated using fundamental bending theory with an applied stress level of $60\%P_u$. The linear regression provided $m = 0.0000594$ and $n = 0.2577$ for the GFRP. The experimentally obtained parameters agreed well with those reported by others (McClure

44

and Mohammadi 1995; Scott and Zureick 1998). The residual moduli of the experimental beams were obtained using Eq. 3.8 and shown in Fig. 3.7, including a trend line equation that was used for modeling. It should be noted that Beam C60-2 was not included in Fig. 3.7 because it exhibited local rotation during the load test and thus stiff deflection was measured (to be discussed). A decrease of 12.4% in residual modulus was observed when the sustained intensity increased from $0\%P_u$ to $60\%P_u$ as per the trend line. Such behavior illustrates the time-dependent material degradation of the GFRP beams, depending upon the level of long-term stress.
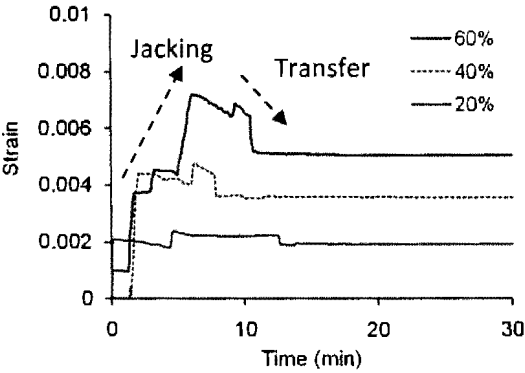
Fig. 3.5. Measured tensile strains at midspan of beams during jacking operation
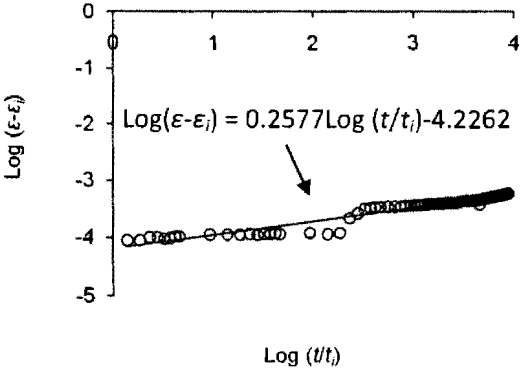
Fig. 3.6. Determination of creep parameters of GFRP (Beam R60-1)

45
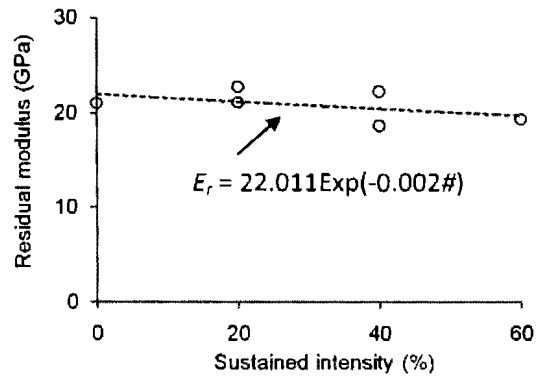
Fig. 3.7. Residual modulus of beams subjected to cold temperature

3.7.2. Time-dependent Behavior

Fig. 3.8. shows the creep strain development of the GFRP beam for 2,000 hours (Beam R60-1). The long-term measurement began after one hour of the load-transfer. The experimental creep strain rapidly increased up to approximately 100 hours and then exhibited an almost constant increment rate, as shown in Fig. 3.8(a). The predicted creep strains using Eq. 3.5 agreed well with those measured [Figs. 3.8(a) and (b)]. The predicted viscoelastic modulus (E_v) of the GFRP subject to room temperature (Eq. 3.7) is compared with the experimental counterpart [Fig. 3.9(a)]. For a comparison purpose, an existing predictive equation was additionally used (Zureick 1998):

$$E_t = \frac{1}{1 + (10 / \beta)t^{0.25}} E_0 \tag{3.9}$$

where β is a material constant and t is the time in year. The predicted modulus using Eq. 3.9 was 3.8% lower than the modulus obtained from Eq. 3.7 at 2,000 hours, even though both methods showed good agreement with the test data [Fig. 3.9(a)]. Such a difference

46

between Eqs. 3.7 and 3.9 is explained by the facts that i) Eq. 3.9 includes an empirical

parameter (β = 60 was used here after Zureick 1998) that has been calibrated in a test

condition having sustained loads less than 30% of the ultimate capacity of GFRP and ii)

Eq. 3.7 is based on curve-fitting (Fig. 3.6). The creep deflection of Beam R60-1 is shown in

Fig. 3.9(b), using the analytical approach described previously. The predicted and

experimental creep deflections increased up to 1.2 mm and 1.3 mm at 2,000 hours (about

10% of the instantaneous elastic deflection), respectively. Despite such good agreement,

some discrepancy was noticed between the creep model and test: the predicted creep

deflection tended to stabilize after 2,000 hours; however, the experimental deflection kept

increasing. This observation implies that the Findley's creep theory tends to underestimate

the creep deflection of a GFRP beam when considerable permanent loads are sustained for

a significant period of time (e.g., 60% of the static capacity over 2,000 hours).

(a)   (b)
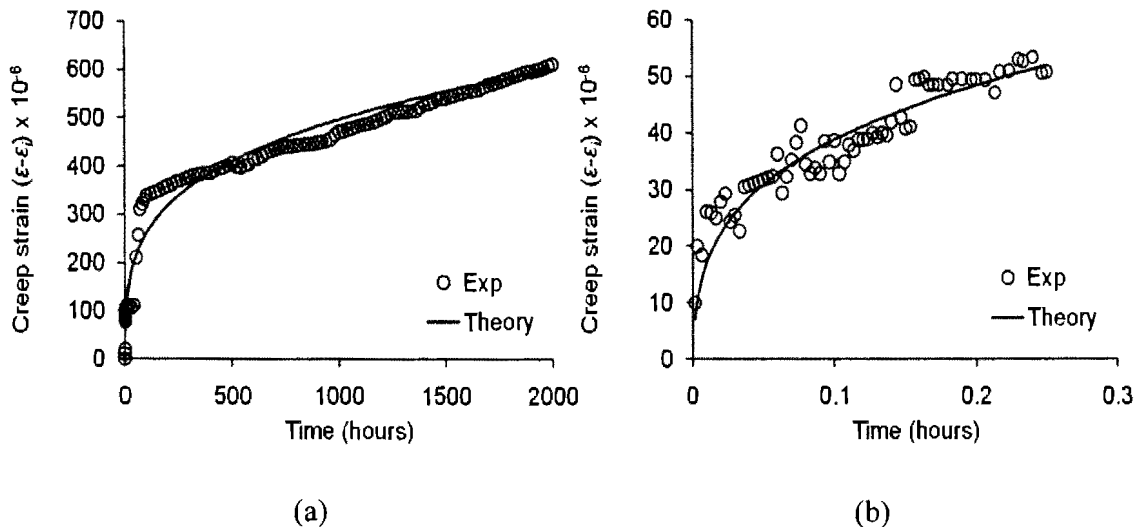
Fig. 3.8. Creep strain versus time (Beam R60-1): (a) up to 2000 hours; (b) close-up view
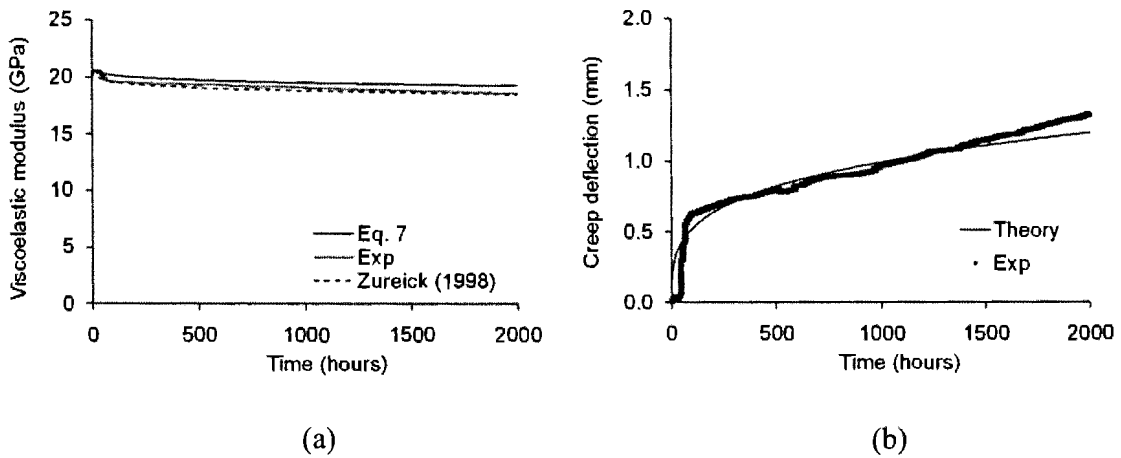
Fig. 3.9. Time-dependent response of GFRP beams (Beam R60-1): (a) longitudinal viscoelastic modulus; (b) creep deflection

3.7.3. Load-carrying Capacity

The load-carrying capacity of all test beams is summarized in Table 3.1, including the residual capacity of the beams subjected to long-term load. The control beam without sustained intensity failed at a load of 31.5 kN. Corresponding FE and analytical beams exhibited ultimate loads of 31.5 kN and 34.7 kN, respectively. The discrepancy in the analytical approach is attributed to the empirical nature of the failure criteria (Eqs. 3.1 to 3.4). It is important to note that these failure equations are not an absolute predictor, but can estimate a critical condition of the beam. The failure of the control beam was due to the fracture of flange near the loading point, followed by fracture crack propagation down the web, as shown in Fig. 3.10(a). The prediction based on the Tsai-Wu failure criterion in the FE beam was similar [Fig. 3.10(b)], while discrete web shear failure was not available due to the continuum modeling method used here. The analytical beam failed primarily due to the flange crushing; however, the web shear failure was also critical, as summarized in Table 3.3 (in fact, these failure modes were expected for all the other beams). The

48

experimental beams (R60-1 and -2) subjected to a sustained intensity of $60\%P_u$ at room temperature showed a decrease of 11.9% in failure load, on average, when compared with the control beam (Table 3.1). Such a decrease is due to the time-dependent material characteristics of GFRP (i.e., dislocation of the constituents induced by long-term loads, Rivera and Karbhari 2001), resulting in weakening of the polymeric chains. The predicted beams (Beam R60) exhibited a similar trend even though the decrease was less pronounced (i.e., 1.3% and 1.4% for the FE and analytical beams, respectively). These discrepancies between the prediction and test are explained by the fact that the residual modulus used for the models (Eq. 3.8) could not accurately represent the time-dependent material characteristics of the GFRP from a microscopic-damage perspective and thus ideal failure loads were achieved. The test beams subjected to sustained loads combined with cold temperature exposure exhibited average decreases of 4.1%, 10.0%, and 16.2% in ultimate load for 20%, 40%, and $60\%P_u$, respectively, as shown in Table 3.1. Similar observations were made for the predicted beams, whereas the load drop due to the sustained intensity was relatively insignificant in comparison to that of the experimental beams. Such an observation is due to the fact that the ultimate load of the FE beam was determined when the Tsai-Wu failure index reached unity [Fig. 3.10(b)], so additional load could not be sustained beyond the critical limit. The analytical beams demonstrated an analogous issue (Table 3.3). The effect of temperature on load-carrying capacity of the GFRP beams subjected to $60\%P_u$ is compared in Fig. 3.11. Although insufficient experimental observations were made to conclude the cold temperature was a significant factor (because of the limited number of test specimens, Table 3.1) the predicted beams obviously showed a trend of decreasing capacities when the temperature decreased. This may be related to

49

Table 3.3. Predicted failure of GFRP beams

Beam	Stress/failure	Lateral torsional buckling σ_{cr}^{LTB}	Flange failure σ_{cr}^{flange}	Web buckling σ_{cr}^{web}	Web shear failure τ_{cr}^{web}
Control	Critical stress	59	210	181	31
	Applied stress	210	210	26	26
	Failure	No[a]	Yes	No	Close
R60	Critical stress	58	207	178	31
	Applied stress	207	207	26	26
	Failure	No[a]	Yes	No	Close
C20	Critical stress	59	211	181	31
	Applied stress	211	211	26	26
	Failure	No[a]	Yes	No	Close
C40	Critical stress	57	203	174	30
	Applied stress	203	203	25	25
	Failure	No[a]	Yes	No	Close
C60	Critical stress	54	193	166	28
	Applied stress	193	193	24	24
	Failure	No[a]	Yes	No	Close

[a]: braces were installed to preclude lateral torsional buckling
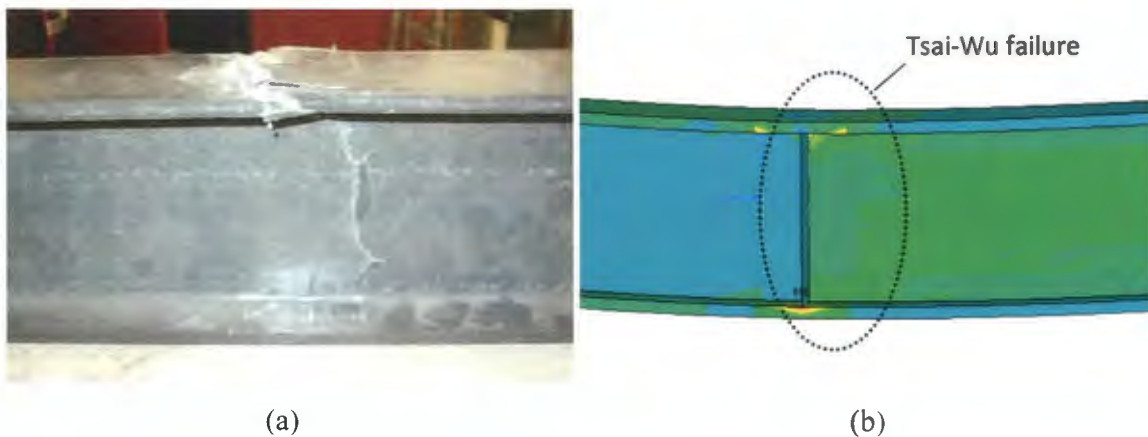
Fig. 3.10. Failure mode of control beam: (a) experiment; (b) model

thermally-induced micro-stresses in the GFRP, accelerating brittle deformation of the constituent material (Dutta and Hui 1996). It is, therefore, recommended that GFRP composites be used with additional care when cold region environments are expected. Further research is necessary to provide strength reduction factors for practicing engineers

with additional microscopic experimental observations, depending upon the level of environmental exposure in cold regions.
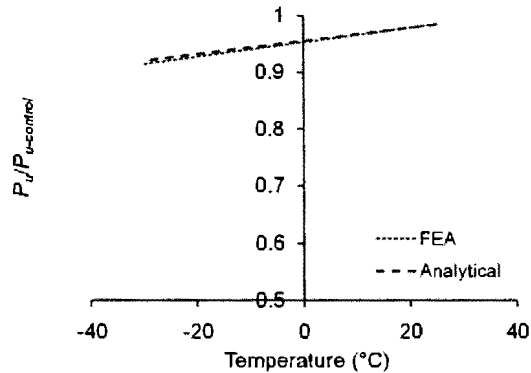
Fig. 3.11. Effect of cold temperature on beams subjecetd to sustained load of 60%P_u

3.7.4. Flexural Behavior

Fig.3.12. shows the midspan load-displacement of the GFRP beams. The experimental control beam exhibited a linear response up to approximately 85% of the ultimate load, followed by a gradual decrease in flexural stiffness until failure occurred [Fig. 3.12(a)]. Such stiffness degradation illustrates local GFRP crushing in the upper flange of the test beam. The experimental beams exposed to cold temperature with various levels of sustained intensities exhibited a similar linear response to the control beam, as shown in Figs. 3.12(b) through (d); however, the gradual stiffness degradation near the failure load was not noticed. This observation confirms the previous explanation as to the accelerated brittleness of the GFRP material when exposed to cold temperature and also implies that the cold temperature effect has altered the constituent characteristics of the GFRP (Nordin et al. 2010). Predicted load-displacement responses showed good agreement with those measured in spite of the ideal linear behavior (Fig. 3.12). In general, the FE beams exhibited relatively stiff responses possibly due to their ideal material characteristics

51

along the loading span. The predicted tensile strains at midspan also agreed with the experimental counterparts, as shown in Fig. 3.12(f): only C40 beams are shown here for brevity. It should be noted that the strain response of the FE beams was compatible to that of the analytical beams because both approaches were only concerned with midspan behavior.

The effect of sustained intensities associated with cold temperature is summarized in Fig. 3.13. The residual capacity of the beams tended to decrease with sustained load levels [Fig. 3.13(a)]. For example, the capacity of Beam C60 decreased by 8.4% and 16.2%, on average, for the prediction and experiment, respectively, when compared to that of the control. The relatively insignificant decrease in the predicted ultimate load is attributed to the empirical failure criteria, as discussed previously. The flexural stiffness of the beams showed a similar trend [Fig. 3.13(b)]. The model prediction was more obvious in addressing the sustained intensity effect because of the ideal flexural behavior based on the estimated residual modulus, Eq. 3.8. It is worthy of noting that the modulus of GFRP materials tends to increase with decreasing temperature without sustained intensities (Dutta and Hui 1996); however, the flexural behavior of GFRP beams is substantially affected by the sustained intensities. Practicing engineers should be aware of these two crucial aspects when pursuing a design project using GFRP in cold region applications. Figure 3.14 evaluates the contribution of shear deformation to the global displacement of the beams at a typical service load level of 18 kN (about 60% of the control capacity), based on the analytical model. The normalized displacement in the y axis of Fig. 3.14 indicates the shear deformation of the long-term beams divided by that of the control. The shear deformation of the GFRP beams was influenced by the level of sustained load and temperature. These

52

observations indicate that the effect of long-term load is a crucial consideration for the serviceability of GFRP beams. To generalize this preliminary conclusion, extensive experimental investigations may be recommended.
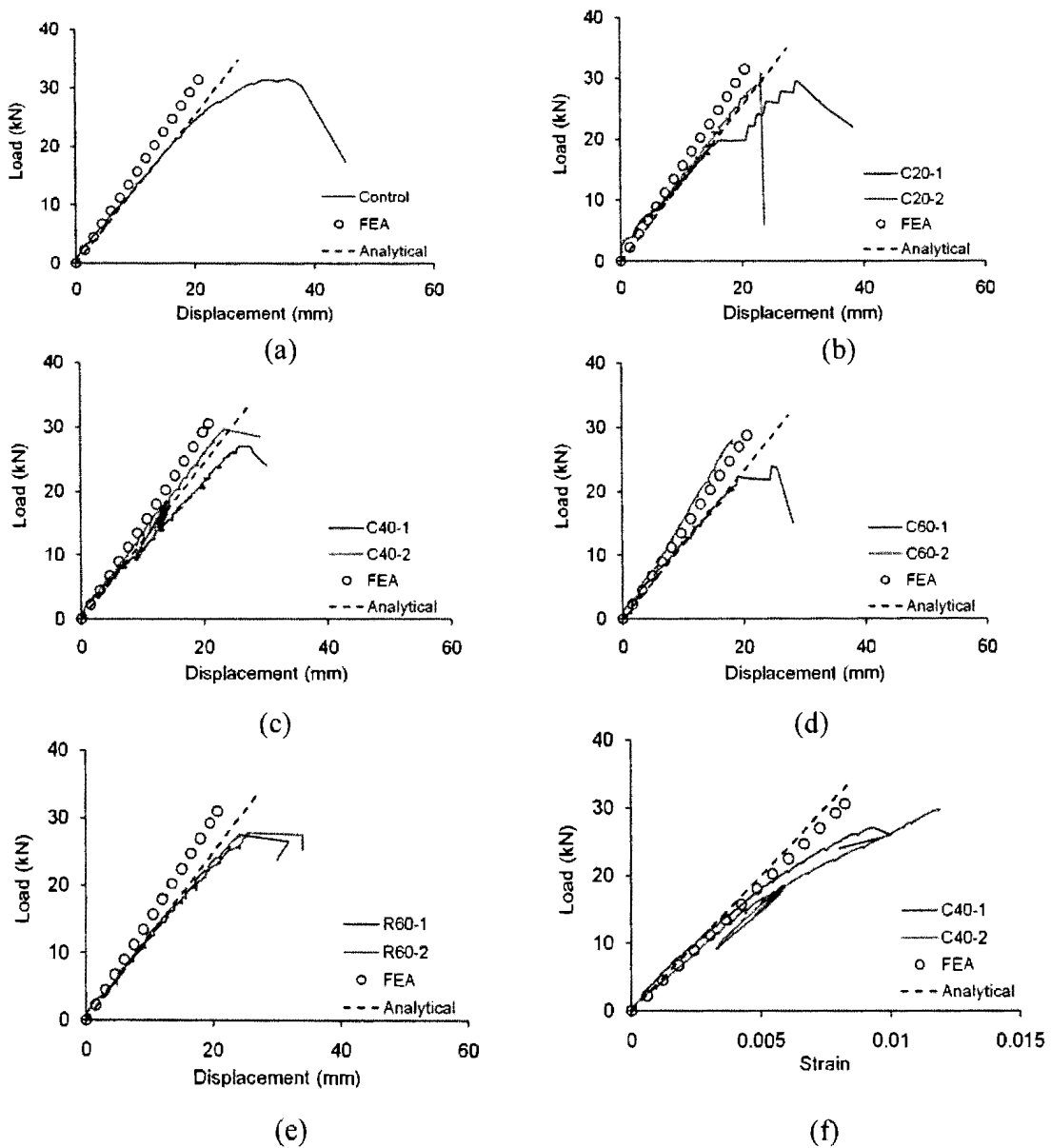
Fig. 3.12. Flexural response of GFRP beams: (a) Control at room (25°C); (b) 20% P_u at 30°C; (c) 40% P_u at -30°C; (d) 60% P_u at -30°C; (e) 60% P_u at 25°C (room); (f) tension strain of 40% P_u at -30°C

53
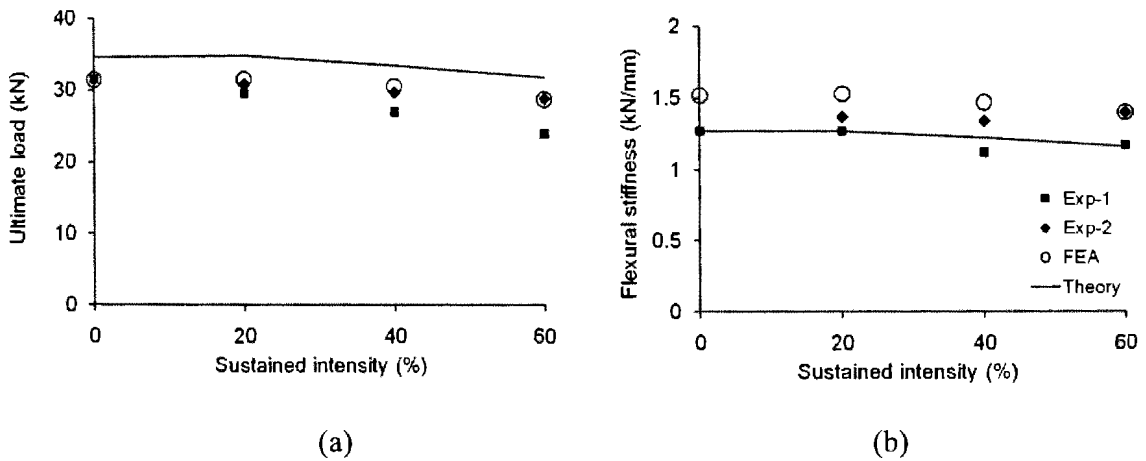
Fig. 3.13. Effect of sustained intensity associated with cold temperature (solid = experimental; hollow = FEA; line = analytical): (a) ultimate load; (b) initial flexural stiffness
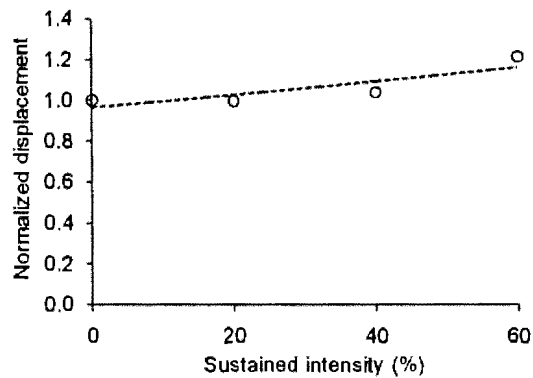
Fig. 3.14. Contribution of shear deformation to midspan displacement at service based on analytical model (circle = individual; line = best-fit)

3.8. PARAMETRIC STUDY

A parametric study was conducted to examine the effect of cold temperature on the behavior of GFRP beams. For this research, the viscoelastic modulus of the GFRP (Eq. 3.7) subjected to long-term load (i.e., $60\%P_u$ providing the measured creep parameters at room temperature, Fig. 3.6) was assumed to be equivalent to the residual modulus (Eq. 3.8) of

the counterpart beam exposed to cold temperature due to the limited instrumentation of the beams located in the environmental chamber. Such an assumption is reasonably accepted when the residual behavior of a structural member is examined (Chowdhury et al. 2008). The material constant n was not sensitive within a range of ±50% of the value measured at room temperature, as shown in Fig. 3.15(a). It was thus assumed that the n value was not influenced by the cold temperature exposure. The extrapolation of the long-term effect over 2,000 hours was not reported here even though the predictive methods agreed well with experimental counterparts. The reason is due to the fact that the Findley's creep theory adopted here exhibited some discrepancy when the time approached 2,000 hours, as previously discussed in Fig. 3.9. Figure 3.15(b) shows the variation of the stress-dependent material constant m that was interpolated from the values obtained from the beams loaded at 60%P_u. Such a linear interpolation with sustained intensity is acceptable by the definition of m, as explained in Eqs. 3.5 through 3.7. The estimated m value of the beam in 60%P_u at cold temperature was 15.4% lower than that at room temperature [Fig. 3.15(b)]. This observation agrees with Dutta and Hui (1996) reporting that the longitudinal modulus of GFRP increased at low temperature (note that m is inversely proportional to the modulus in Findley's theory). The variation of viscoelastic modulus of the GFRP is shown in Fig. 3.16(a). The degradation of the modulus was gradual and converged after 1,500 hours. The average decrease in modulus was 7.3% and 8.2% for the GFRP subjected to cold and room temperatures, respectively, from 0 to 2,000 hours [Fig. 3.16(a)]. The predicted creep strain of the GFRP beams in various levels of long-term load is shown in Fig. 3.16(b). The effect of cold temperature was more obvious when the sustained intensity increased. The difference in creep strain between the beams exposed to room and cold temperatures at

2,000 hours was 30.8, 61.6, and 92.3 microstrains for 20%P_u, 40% P_u, and 60% P_u, respectively. These low creep strains at low temperature may be beneficial for GFRP beams in cold region applications, whereas the change of weather can cause environmental fatigue because of the different long-term characteristics in cold and mild temperatures.

(a)   (b)
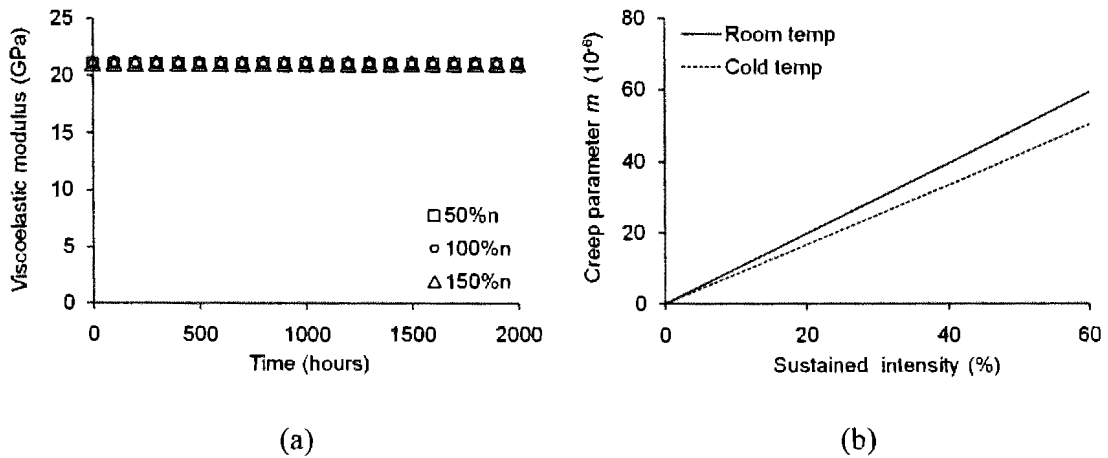
Fig. 3.15. Long-term properties for parametric study: (a) sensitivity analysis of creep paramater n; (b) predicted creep parameter m

(a)   (b)
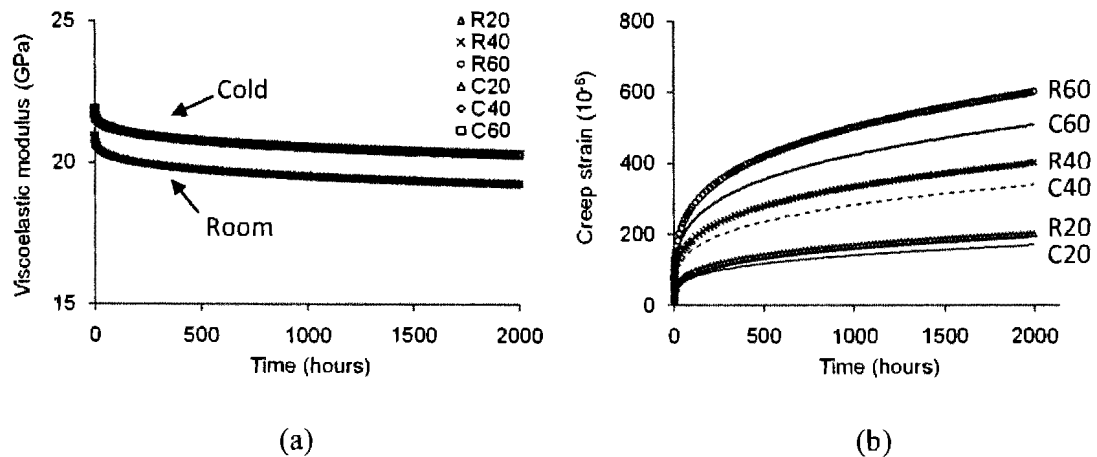
Fig. 3.16. Parametric study on cold temperature effect: (a) viscoelastic modulus; (b) creep strain

56

3.9. SUMMARY AND CONCLUSIONS

- The experimental strains of the GFRP beams stabilized in 15 minutes after load-transfer and gradually increased up to 2,000 hours. The predicted approaches showed good agreement with those measured. The experimentally-obtained residual modulus decreased when the sustained intensity increased, representing time-dependent material degradation. An empirical equation was proposed to predict the long-term characteristics of GFRP for cold region applications. Findley's theory tended to underestimate the creep deflection of the beam subjected to $60\%P_u$ over 2,000 hours.

- The effect of sustained intensities associated with cold temperature ($-30°C$) was noticeable on the load-carrying capacity of the GFRP beams. The experimental beams failed due to the flange crushing, followed by web shear fracture induced by crack propagation. The predicted beams showed a similar failure mode. The proposed residual modulus approach to predict the behavior of the GFRP beams in long-term load was reasonably acceptable; however, further development may be necessary for better prediction by taking into account time-dependent micro-structural responses of GFRP materials.

- Cold temperature exposure accelerated the brittle behavior of the GFRP beams, in particular noticeable when sustained intensities were accompanied, based on the fact that gradual local GFRP crushing was not observed for the beams in the long-term loads. The shear deformation of the GFRP beams increased with sustained loads.

- The effect of cold temperature altered the creep response of the GFRP beams, in particular significant when the level of sustained intensity increased. The contribution of the creep parameter n to the viscoelastic modulus was not noticeable at cold temperature.

3.10. REFERENCES

ASTM. 2010a. Standard test method for surface burning characteristics of building materials, American Society for Testing and Materials, West Conshohocken, PA.

ASTM. 2010b. Standard test methof for rate of burning and/or extent and time of burning of plastics in a horizontal position, West Conshohocken, PA.

Bai, Y. and Keller, T. 2009. Time dependence of material properties of FRP composites in fire, Journal of Composite Materials, 43(21), 2469-2484.

Bank, L.C. 1987. Shear coefficient for thin-walled composite beams, Composite Structures, 8, 47-61.

Bank, L.C. 2006. Composites for construction, John Wiley & Sons, Hoboken, NJ.

Bank, L.C. and Mosallam, A.S. 1992. Creep and failure of a full-size fiber-reinforced plastic pultruded frame, Composites Engineering, 2(3), 213-227.

Chowdhury, E.U., Bisby, L.A., Green, M.F., and Kodur, V.K.R. 2008. Beams prestrengthened in flexure with fiber-reinforced polymer sheets, Journal of Composites for Construction, 12(1), 61-68.

Deskovic, N., Triantafillou, T.C., and Meier, U. 1995. Innovative design of FRP combined with concrete: short-term behavior, Journal of Structural Engineering, 121(7), 1069-1078.

Dutta, P.K. and Hui, D. 1996. Low-temperature and free-thaw durability of thick composites, Composites Part B, 27(3-4), 371-379.

Dutta, P.K., Lopez-Anido, R., and Kwon, S.K. 2007. Fatigue durability of FRP composite bridge decks at extreme temperatures, International Journal of Products and Technology, 28(1/2), 198-216.

Findley, W.N. 1960. Mechanism and mechanics of creep of plastics, SPE Journal, 16, 57-65.

58

Keller, T., Bai, Y., and Vallee, T. 2007. Long-term performance of a glass fiber-reinforced polymer truss bridge, Journal of Composites for Construction, 11(1), 99-108.

McClure, G. and Mohammadi, Y. 1995. Compression creep of pultruded E-glass-reinforced-plastic angles, Journal of Materials in Civil Engineering, 7(4), 269-276.

Neto, A.B. S.S. and Rovere, H.L.L. 2007. Flexural stiffness characterization of fiber reinforced plastic pultruded beams, Composite Structures, 81, 274-282.

Nordin, C., Ma, Z.J., and Penumadu, D. 2010. Combined effect of loading and cold temperature on the stiffness of glass fiber composites, Journal of Composites for Construction, 14(2), 224-230.

Rivera, J. and Karbhari, V.M. 2001. Characterization of sub-zero response of vinylester FRP in civil infrastructure renewal, 11th International Offshore and Polar Engineering Conference, 124-130.

Roberts, T.M. and Masri, H.M.K.J.A.H. 2003. Section properties and buckling behavior of pultruded FRP profiles, Journal of Reinforced Plastics and Composites, 22(14), 1305-1317.

Scott, D.W. and Zureick, A.H. 1998. Compression creep of a pultruded E-glass/vinylester composite, Composites Science and Technology, 58, 1361-1369.

Shao, Y. and Shanmugam, J. 2004. Deflection creep of pultruded composite sheet piling, Journal of Composites for Construction, 8(5), 471-479.

Strongwell. 2009. FRP specifications: section 06600 fiberglass reinforced polymer products and fabrications, Bristol, VA.

Tsai, S.W. and Wu, E.M. 1971. A general theory of anisotropic materials, Journal of Composite Materials, 5, 58-80.

Zureick, A. 1998. FRP pultruded structural shapes, Progress in Structural Engineering and Materials, 1(2), 143-149.

CHAPTER 4. SHORT- AND LONG-TERM RESPONSES OF CONCRETE BEAMS STRENGTHENED WITH NSM CFRP COMPOSITES: EXPERIMENTAL INVESTIGATIONS

4.1. SYNOPSIS

This chapter represents the short and long-term behavior of reinforced concrete beams strengthened with near surface mounted (NSM) fiber reinforced polymer (FRP) strips subjected to different loading conditions. FRP composites consist of high-strength fibers embedded in an epoxy resin and provide high strength to weight ratio and durability. A total of thirteen beams were tested under monotonic loads where eight beams were tested to get residual capacity after removal of sustained intensities. The long-term beams were subjected to three levels of sustained intensities (25%, 50%, and 75% of the static capacity) at room (25°C) temperature for 4,000 hours. In addition, three specimens were cyclically loaded to evaluate low-cyclic fatigue performance. All the beams were tested in four points bending to study the effect of long-term sustained intensities on flexural behavior, failure modes, and crack patterns. Experimental results reveal that both the load carrying capacity and failure modes were influenced by the level of sustained intensities and cyclic loads.

4.2. INTRODUCTION

The necessity to strengthen civil infrastructures is a major crisis for building owners. Under-performing structures are usually strengthened by fiber reinforced polymer (FRP) sheets or plates bonded on the external surface (Al-Mahmoud et al. 2009). The near surface mounted strengthening technique is not a new method which is being used since 1948 (De Lorenzis et al. 2000). The invention of epoxy, which has a very high adhesive

strength, moisture tolerance, negligible shrinkage and wide range of viscosity, makes a remarkable contribution to the rehabilitation process in late 1960s (Täljsten and Carolin 2001; Hassan and Rizkalla 2003). Carbon FRP (CFRP) materials exhibits high strength, light weight, noncorrosive properties and ease of applications with minimum maintenance cost (Bakis et al. 2002; Kim et al. 2005; Kim and Heffernan 2008; Kim et al. 2008b). McKenna (1993) investigated the use of CFRP to strengthen reinforced concrete beams under monotonic loading. Significant increase in flexural capacity due to strengthening was observed in their experiment. Brena et al. (2003) studied the increase in the flexural capacity of RC beams strengthened with CFRP composites. Their test result showed a stiffer response of strengthened beam than their companion control beam. Among all retrofitting techniques NSM shows improved bond performance when compared to externally-bonded CFRP composites (Seracino et al. 2007).

The level of service load on bridge structures has significantly increased now a days. Cyclic vehicle load is a major concern in designing a bridge structure to ensure the structural stability. Most of the investigations carried out under cyclic load have been focused on studying fatigue phenomena which are characterized by high number of cycles (eg. Harries and Aidoo 2006; Harries et al. 2006; Harries et al. 2007; Kim and Heffernan 2008). On the contrary, this research is executed under low number of cycles to put the effect of live load during construction period. This live load represents the traffic and equipment loads on bridge during the operation period. Due to lack of design indication about the effect of low cyclic load on the overall behavior of NSM beams more research should be conducted in this area.

The majority of the studies mentioned above have focused on the short-term characteristics of concrete beams strengthened with FRP composites. Creep analysis of a concrete body depends on various factors such as concrete strength, the composition of the concrete, water contents, the dimensions of the element (ACI 209R). With the passes of time, when a material is under sustained loading, the material acquires a meta-stable condition where it seems stable but a small change of loading condition can make it unstable consequently failure can happen. Plevris et al. 1992 developed a fundamental understanding of the time-dependent (creep and shrinkage) behavior of reinforced-concrete beams strengthened with FRP laminates. They used an analytical model to predict the deflection of concrete beams strengthened with FRP laminates having different thicknesses and they confirmed the theoretical analysis by comparing with their experimental findings. Shin and Lee (2003) investigated the flexural behavior of FRP strengthened reinforced concrete beam at different level of sustained loads. They developed a theoretical model based on displacement-controlled nonlinear finite element analysis to predict this flexural behavior. Savoia et al. (2005) studied creep deformation of FRP-plated reinforced concrete tensile members. Their study indicates the increase in stiffness and reduction of crack width due to the application of FRP plate in the tensile members. Tan and Saha (2006) studied, both analytically and experimentally, the long-term deflection characteristics of FRP-bonded beams under sustained loads. Chami et al. (2009) tested beams strengthened with externally bonded CFRP sheets where they found that the long term effect of the FRP was not significant for deflection control, this may be due to the fact that the major creep strain typically occurred in the compression side of the beam however the flexural strengthening and crack control behavior was achieved by the strengthening schemes.

Although some research has been conducted in the area of strengthening of reinforced concrete structures the fatigue and long-term performance of NSM beams under service loads is still a concern. Deformations due to creep and shrinkage are usually several times larger than instantaneous deformation in concrete structures. Also the time dependent bond performance of NSM beams needs to be investigated. This chapter presents the experimental outcomes of NSM beams under cyclic and sustained loading.

4.3. RESEARCH SIGNIFICANCE

The use of NSM CFRP strip for strengthening reinforced concrete structure has been studied under sustained and cyclic loading conditions. The strengthening techniques enhanced the structural capacity consequently but this flexural capacity decreases when subjected to sustained loading. The application of low cyclic load may influence the strength and failure mode of the structural member. Thus, the cyclic and time-dependent behavior of the beams strengthened with NSM CFRP strips needs to be evaluated to avoid structural failure. Very limited information is available on the cyclic and time-dependent behavior of NSM CFRP beams. Therefore, current research reports on the variation of residual strength and failure modes due to cyclic and long-term loading after strengthening the structure.

4.4. EXPERIMENTAL PROGRAM

4.4.1. Beam Details

A total of sixteen beams were tested, where eight were subjected to three levels of sustained loads and the remaining beams were tested under monotonic and cyclic loading conditions, as shown in Table 4.1. Cyclic load was applied by loading and unloading at

every 10 kN. All the beams were comprised of four types of materials such as concrete, steel, CFRP, and adhesive. The concrete mix was designed with a specified compression strength of 20 MPa. The size of the beam was medium which had a length of 1300mm and a cross-section of 100mmx165mm [Fig.4.1]. All test beams were reinforced with 2-#3 longitudinal steel bars($A_s = 71.25$ mm^2 each) with a specified yield strength of 414MPa. The distance of double leg stirrup was 75mm and #2 steel bars($A_s = 31.66$ mm^2 each) were used as shear reinforcement. A groove was cut at the tension face to insert the CFRP strip and ACI 440 guideline was followed for the groove dimension of the specimens [Fig.4.2].

Table 4.1. Beam details

Beam	NSM CFRP layer	Bonding agent	Load type	Load (kN)[a]			Failure mode[a,b]
				P_{cr}	P_y	P_u	
Control	0	None	Monotonic	9.2	38.0	39.5	CC
SE0(1)-1	1	Epoxy	Monotonic	11.4	50.3	67.5	IC
SE0(1)-2	1	Epoxy	Cyclic	11.3	51.4	75.8	DE
SE0(2)-1	2	Epoxy	Monotonic	12.4	53.4	70.1	DE
SE0(2)-2	2	Epoxy	Cyclic	12.4	55.0	65.4	DE
SC0(1)-1	1	Cement-grout	Monotonic	8.6	50.9	57.6	IC
SC0(1)-2	1	Cement-grout	Cyclic	9.5	51.9	60.2	IC
SG(1)-1	1	Geopolymer	Monotonic	9.5	50.4	53.6	IC
LE25(1)-1	1	Epoxy	Sustained at 25%	N/A[c]	49.2	59.6	DE
LE25(1)-2	1	Epoxy	Sustained at 25%	N/A[c]	49.5	58.1	DE
LE50(1)-1	1	Epoxy	Sustained at 50%	N/A[c]	44.7	53.2	DE
LE50(1)-2	1	Epoxy	Sustained at 50%	N/A[c]	44.8	53.9	DE-S
LE50(2)-1	2	Epoxy	Sustained at 50%	N/A[c]	47.4	53.3	DE
LE50(2)-2	2	Epoxy	Sustained at 50%	N/A[c]	50.3	58.4	DE
LE75(1)-1	1	Epoxy	Sustained at 75%	N/A[c]	34.5	38.5	DE-S
LE75(1)-2	1	Epoxy	Sustained at 75%	N/A[c]	37.6	46.8	DE-S

[a]: residual behavior for long-term beams
[b]: CC = concrete crushing; IC = interfacial failure between concrete and NSM CFRP; DE = debonding of CFRP at its end; DE-S = end debonding with significant interfacial bond deterioration
[c]: cracked during jacking operation
Notation: S = short-term; L = long-term; E = epoxy; C = cement-grout; G = geopolymer; 0, 25, 50, 75 = level of sustained load (%), 1 and 2 = repetition of test

According to ACI440 the groove dimensions are a function of the width and cross sectional

area of the strip. The CFRP strip, 16mm wide x 2mm thick, included a tensile strength of

2,068 MPa with a tensile modulus of 124GPa (Hughes Brothers 2009).A predamaged beam

was not used because the retrofitted beam was compared with an identical benchmark

specimen. It is also difficult to get an identical damaged beam because for different

structure in practical field the level of damage may be different during service period. The

bonding agent used in the experiment can be categorized as epoxy, cement-grout, and

geopolymer [Fig.4.3]. Two dog-bone coupons, as shown in Fig.4.4, were made with epoxy

T308 and loaded in tension until failure occurred. This test was arranged to get the

adhesive properties as the manufacturer data were not available.
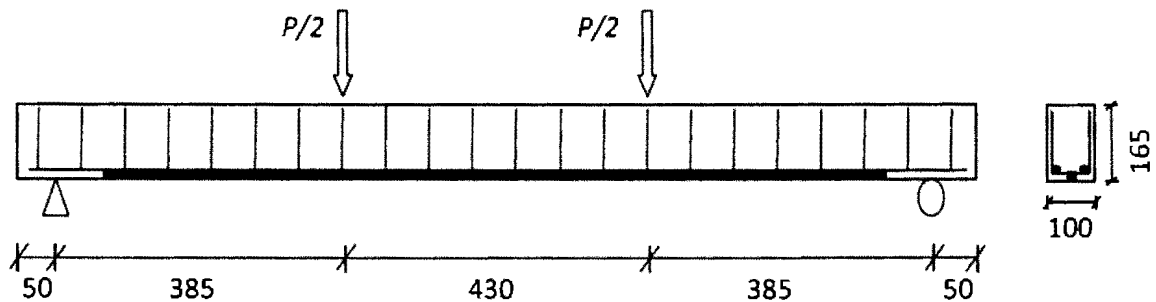
Fig.4.1. Beam details (unit in mm)
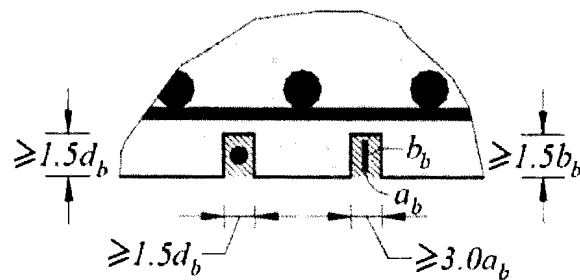
Fig.4.2. ACI 440 prescribed NSM groove dimensions (ACI 2007)
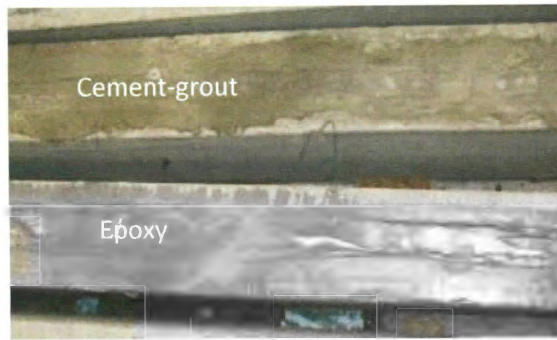
Fig.4.3.Various bonding agents for NSM CFRP
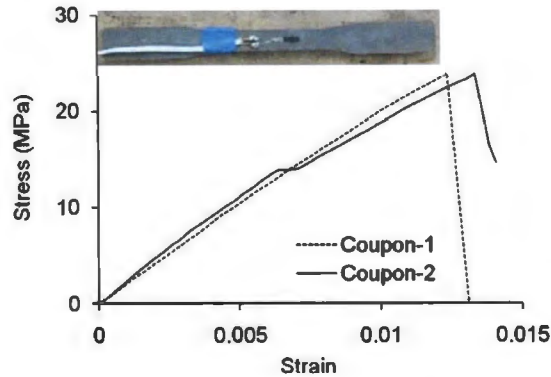
Fig.4.4. Ancillary test: epoxy coupon

4.4.2. Adhesive Properties

The function of groove filler adhesives is to transfer stress between the CFRP strip and concrete. The most important properties of these adhesives are tensile and shear strength. The tensile strength is essential when the beam is subjected to high circumferential tensile stress and the shear strength is required when the bond is controlled by cohesive shear failure of the epoxy. Tension tests were carried out to find the adhesive properties. Two epoxy coupons were tested and the observed ultimate strength was 23.9 and 23.8 MPa [Fig.4.4]. The coupons failed at the reduced cross section and the stress was determined by dividing the applied load by this reduced cross section (11 mm x 5 mm).

66

From their stress-strain curve, the elastic modulus of the epoxy material was obtained and the obtained modulus was 2008.3 and 1860.6 MPa respectively. The compressive strength of three cement-grout cubes was 31.5, 31.9, and 30.5 MPa with a poisson's ratio of 0.29. The cement-grout has some advantages such as it is cheaper, applicable in wet surfaces and elevated temperature, less hazardous to worker an environment and compatibility with concrete.

4.4.3. Sustained Load

A specially designed steel frame with a hydraulic jack was used for the application of long-term load to the beams in four-point bending [Fig.4.5]. Each frame consisted of a clamping system made of hollow square steel sections (50 mm × 50 mm) with Φ9.5 mm threaded rods and it accommodated two beams subjected to the same sustained loading. The levels of sustained load were 25%, 50%, and 75% of the load-carrying capacity (P_u) of the static control beam (Table4.1). An epoxy adhesive T308 was used as a bonding agent

(a)   (b)
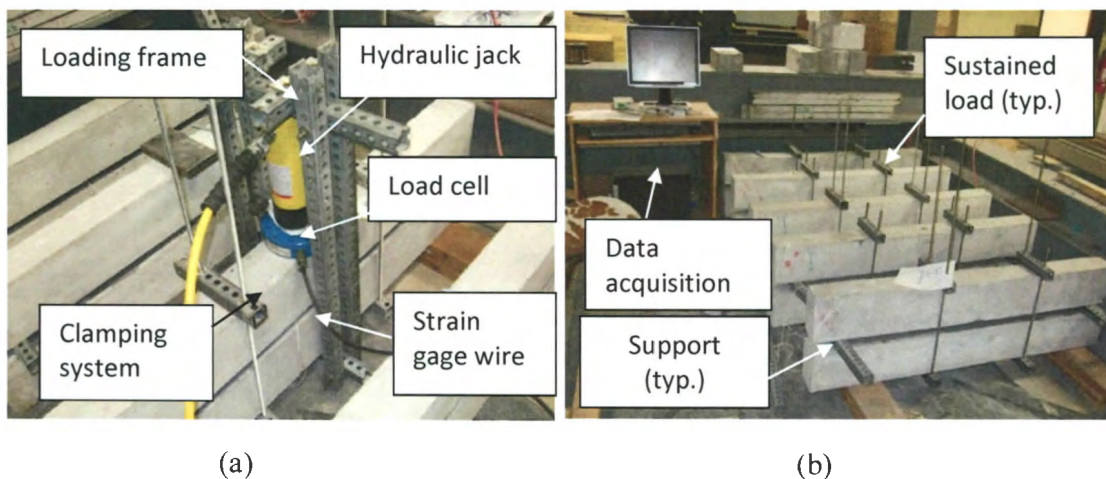
Fig.4.5. Application of long-term load: (a) jacking operation; (b) after load-transfer and strain monitoring

for all long-term beams. A strain gage was attached internally to the CFRP strip at midspan to monitor the variation of strain during the period of sustained intensities. The strain gage was connected with a data acquisition system for recording the variation of strain up to 4,000 hours. The crack propagation was marked with a marker on the beams side face to observe the effect of sustained intensities [Fig. 4.6].

(a)   (b)   (c)
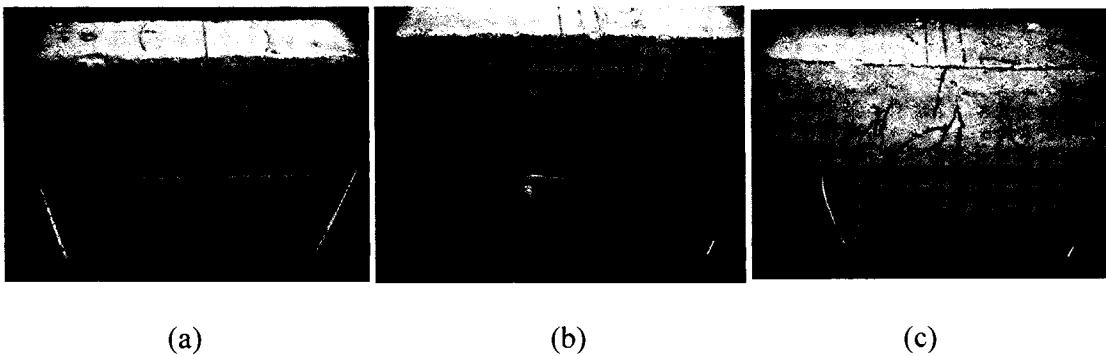
Fig.4.6. Crack formation of long-term beams after 3,000 hours of load-transfer: (a) 25%P_u; (b) 50%P_u; (c) 75%P_u

4.4.4. Test Schemes

All beams were loaded in four-point bending with a span length of 1200mm. These beams were made by pouring the concrete mix into prefabricated steel form. Foams with a dimension of 13.5mmx25mm were used at the bottom of the steel cage to secure the space for CFRP strips. The fabricated concrete beams were moisture-cured for a minimum of 28 days. Before inserting the CFRP strip, the foam was completely removed and the groove surfaces were cleaned with a metal brush. A specially designed mixing nozzle was used to uniformly mix the epoxy adhesive prior to bonding the CFRP strips in the concrete specimen [Fig.4.7]. The cement-grout and geopolymer were manually injected into the groove of the test specimens. The concrete surface was leveled after inserting the CFRP

68

strip into the groove that had been filled with the bonding agents. The curing time for the epoxy adhesive and the cement-grout was approximately one day and seven days, respectively. During the short-term load test the beams were loaded in both cyclic and monotonic conditions until failure occurs. A two legged spreader was used to bring the beam under a four point bending condition [Fig.4.8]. Steel plates of 50mm width were placed underneath the both legs of the spreader to avoid the stress concentrations. A manually operated hydraulic pump was used to apply incremental loads on the beam. A load cell was placed in between the hydraulic jack and spreader to monitor the level of the applied load. A linear potentiometer (LP) was positioned at midspan of each beam to measure vertical displacement. The LP was able to measure a vertical deflection up to 108mm. All test data were recorded by a data acquisition system. PI gauges of 100mm length were installed on top and bottom face of the beams at mid-span. The top and bottom PI gauges were located 15mm below the top face and 15mm above the bottom face. The PI gauges were able to measure a strain ranging from -2.3% to 2.3%. The epoxy coupons were prepared by pouring the liquid epoxy T308 in a mold. After drying, these coupons were removed from the mold and a strain gage was attached at the center [Fig.4.9]. This strain

(a)   (b)   (c)
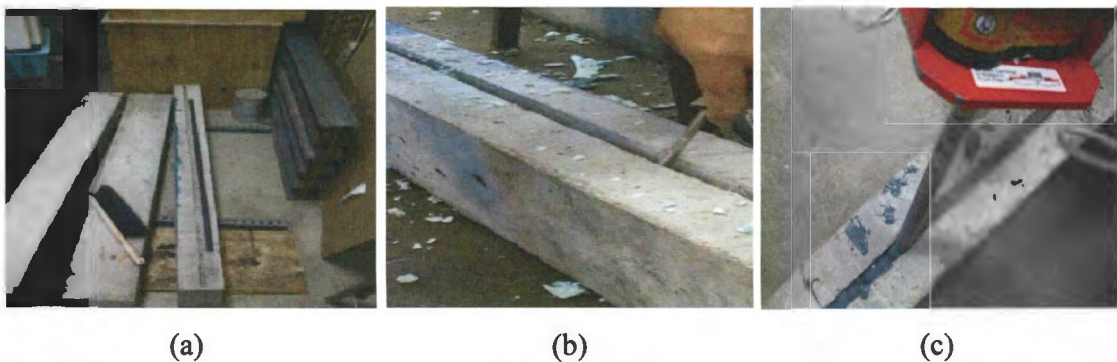
Fig.4.7. CFRP strip installation: (a) groove cleaning; (b) groove preparation; (c) epoxy injection

gage was connected with a strain indicator [Fig.4.9]. These coupons were tested in a servo-hydraulic MTS machine [Fig. 4.9], which has a capacity of 25 kN and a maximum displacement of 100 mm, with a loading rate of 0.25mm/min. The load was measured using a computer system and corresponding strains were recorded using the strain indicator.
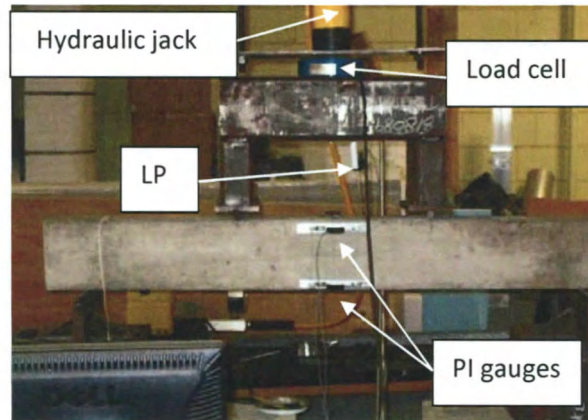
Fig.4.8. Short-term flexural test

(a)   (b)

Fig.4.9. Epoxy coupon test setup: (a) coupon connected with strain indicator; (b) MTS machine

4.5. TEST RESULTS AND DISCUSSION

4.5.1. Short-term Flexural Test

The flexural characteristics of all specimens with different bonding agents in monotonic and cyclic loads are listed in Table 4.1. The ultimate load-carrying capacities after cyclic loading were very close to those of the monotonic loading condition. All the NSM beams showed higher strength due to strengthening with CFRP strips but the variation of strength and failure modes were observed among the beams with different adhesives. The beam with the epoxy adhesive showed a higher load-carrying capacity than those with the cement-grout and geopolymer. The application of epoxy in NSM beams increased the strength about 20% than cement-grout and approximately 30% than geopolymer. The strength of the two layers NSM beams did not increase significantly compared to one layer NSM beams due to inserting additional CFRP layer using epoxy adhesive. Fig.4.10 represents the load versus mid-span deflection of five types of beams Control, SE0(1), SE0(2), SC0(1) and SG0(1). Two stages were observed in the load-deflection curve for the control beam during the increase in positive bending moment but when it was strengthened with NSM CFRP strip, three stages were distinguished on the load versus deflection curve: i) the linear elastic stage which corresponded to the behavior before concrete cracking, ii) concrete cracking to steel yielding stage which was due to increasing of moment until yielding of the steel bar. In this stage, cracking developed according to the applied load and many distributed narrow cracks were observed along the whole length. After stabilizing the concrete cracks, the increment of moment caused the steel bars to yield, and iii) steel yielding to a failure stage where CFRP strips controlled the crack width after yielding of the steel. All the strengthened beams displayed bending

behavior similar to the unstrengthened beam up to cracking which indicates the insignificant contribution of CFRP strip to the increase in the overall stiffness of the beam within the elastic range. However, a significant increase in stiffness and strength was observed after cracking of the beams. Development of tensile strain for control, SE0(1)-1, SE0(2)-1, SC0(1)-1 and SG(1)-1 beam has been shown in Fig. 4.11. The effective moment of inertia also changes with the change of the neutral axis. The stress and strain was linear up to yielding of the steel; hence, the elastic theory is valid up to that point. The deflection is a function of applied load P and EI. A back-calculated method was used based on Eq.4.1 to compute the effective moment of inertia.

$$I_e = \frac{Pa(3l^2 - 4a^2)}{48E_c\delta}$$

(4.1)

Where P is the applied load and δ is corresponding deflection,I_e is the effective moment of inertia of the beam, and E_c is the modulus of the concrete. The length from the support of the concrete beam to the loading point is a and l is the span length of the beam. The variation of effective moment of inertia with respect to load and comparison between the beams bonded using epoxy, cement-grout, and geopolymer are represented in Fig. 4.12. Initially I_e was constant up to a range of 12~15kNfor all the beams and then it started to decrease. The effective moment of inertia I_e degraded more for the control beam for all cases. I_e of beam SE0(1)-1 decrease less than that of SE0(2)-1 [Fig.4.12(a)] whereas I_e for beam SG(1)-1 decreased more than that of SC0(1)-1[Fig.4.12(b)].

72
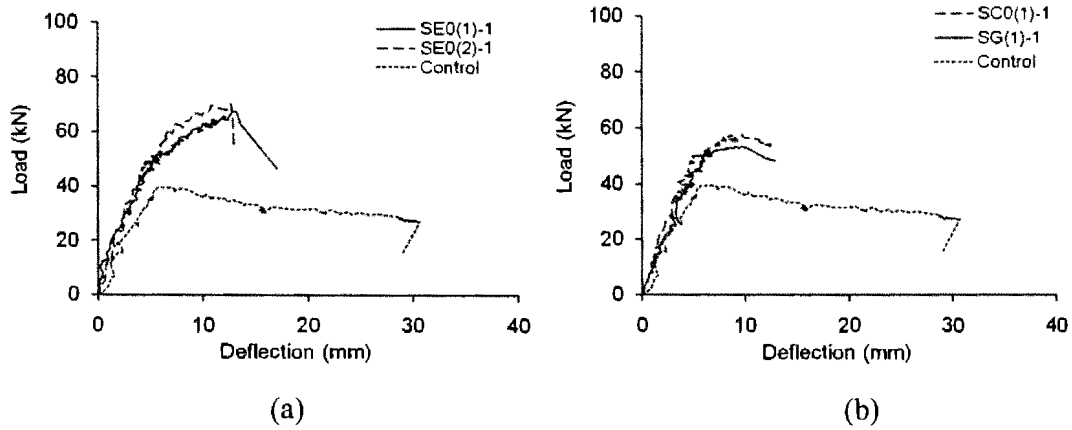
Fig.4.10. Load-displacement behavior of short-term beams: (a) CFRP strips with epoxy adhesive; (b) CFRP strips with cementitious resins
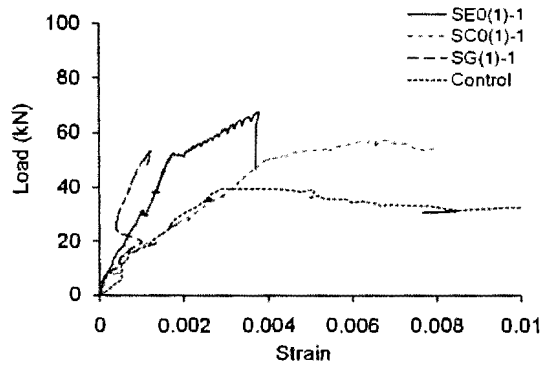
Fig.4.11. Development of tensile strains
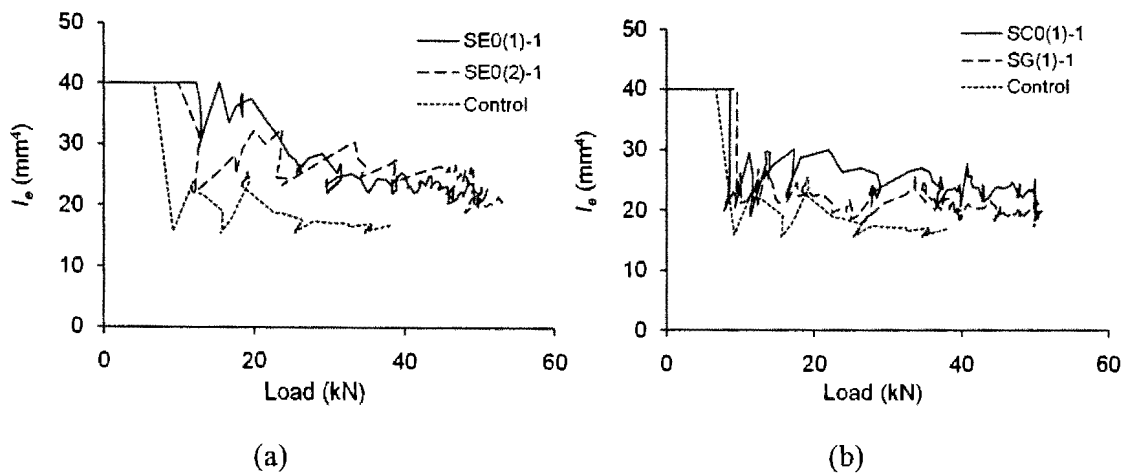
Fig.4.12. Effective moment of inertia: (a) CFRP strips with epoxy adhesive; (b) CFRP strips with cementitious resin

73

4.5.2. Time-dependent Behavior of NSM Beams

Fig.4.14. shows the variation of creep strain of the CFRP strip for 4,000 hours. Six beams with one layer NSM CFRP strip were subjected to three levels of sustained intensities (25%, 50% and 75% of its ultimate capacity) and one pair of beams with two-layer NSM CFRP strips was subjected to 50% sustained load. The CFRP strips were bonded with an epoxy adhesive for all long-term beams. During jacking the strain went up to a certain level and became constant after transfer [Fig.4.13]. When the desired level of load was achieved, the threads were tightened from both sides to hold the level of sustained intensities. All the beams cracked during the jacking operation and significant cracking was observed for the beam with 75% sustained load. For all the beams under sustained loads, degradation of CFRP strains with respect to time was observed due to the deterioration of bonding between the CFRP strip and epoxy adhesive. Bond deterioration decelerates the composite action between concrete and CFRP strip. As a result slippage occurs and the CFRP strain reduced. From Fig.4.6 it can be seen that at a load level of $75\%P_u$ there were
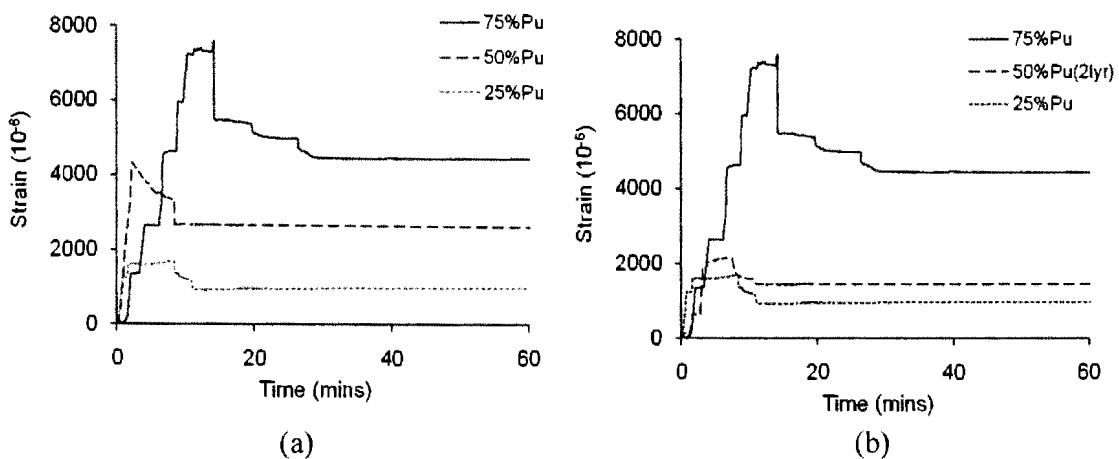
Fig.4.13. Jacking operation and load transfer of beams: (a) 1-layer NSM CFRP; (b) 2-layer NSM CFRP

74

many flexural cracks as well as a shear crack near the ends and for 50% P_u there were very few flexural cracks at midspan whereas there were very few visible cracks at the time of loading for 25%P_u and hair cracks were observed with time.
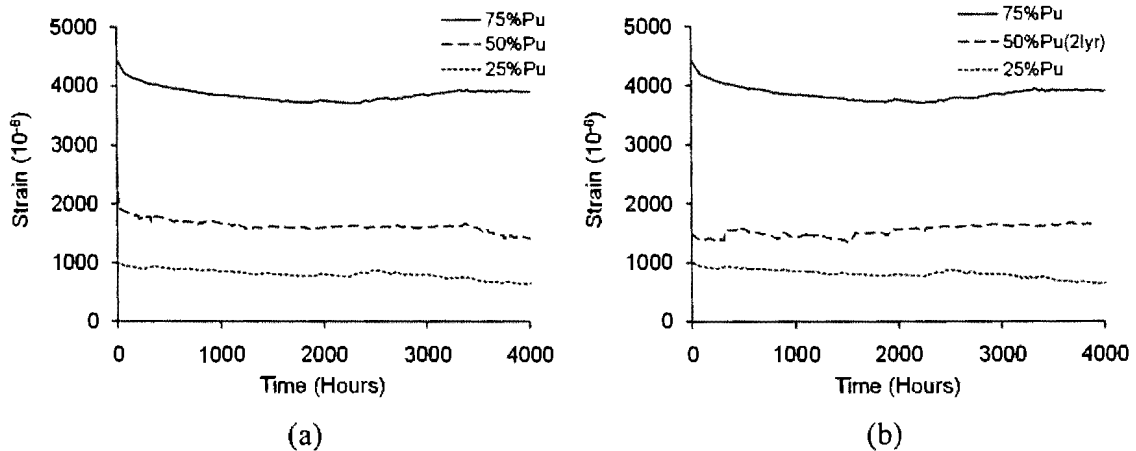
Fig.4.14. Long-term CFRP strains: (a) 1-layer NSM CFRP; (b) 2-layer NSM CFRP

4.5.3. Residual Load-carrying Capacity

The residual capacity of the long-term beams was summarized in Table 4.1. To explain the time-dependent effect, beam SE0(1)-1 was considered as a control beam for these cases. Each beam was loaded monotonically until failure to obtain the ultimate residual capacity and a decrease in ultimate load-carrying capacity was observed due to the increase in the level of sustained intensities. The effect of sustained intensities on load-carrying capacity is compared in Fig.4.15. The test beams subjected to sustained loads exhibited average decreases of 12.5%, 21.4%, and 39.2% in ultimate load for 25%, 50%, and 75%P_u, respectively, as shown in Table4.1. In case of beams with two layers of CFRP strip, the reduction was about 18.5% in ultimate load for 50%P_u. The long-term beams also exhibited the similar three stage load-deflection behavior as described in Section 4.5.1. A

lower value of stiffness and ultimate deflection was observed in the long-term beams. The NSM beam exhibits maximum load carrying capacity a debonding failure. After debonding failure load-deflection curve gradually decrease until concrete crushed at its compression zone.
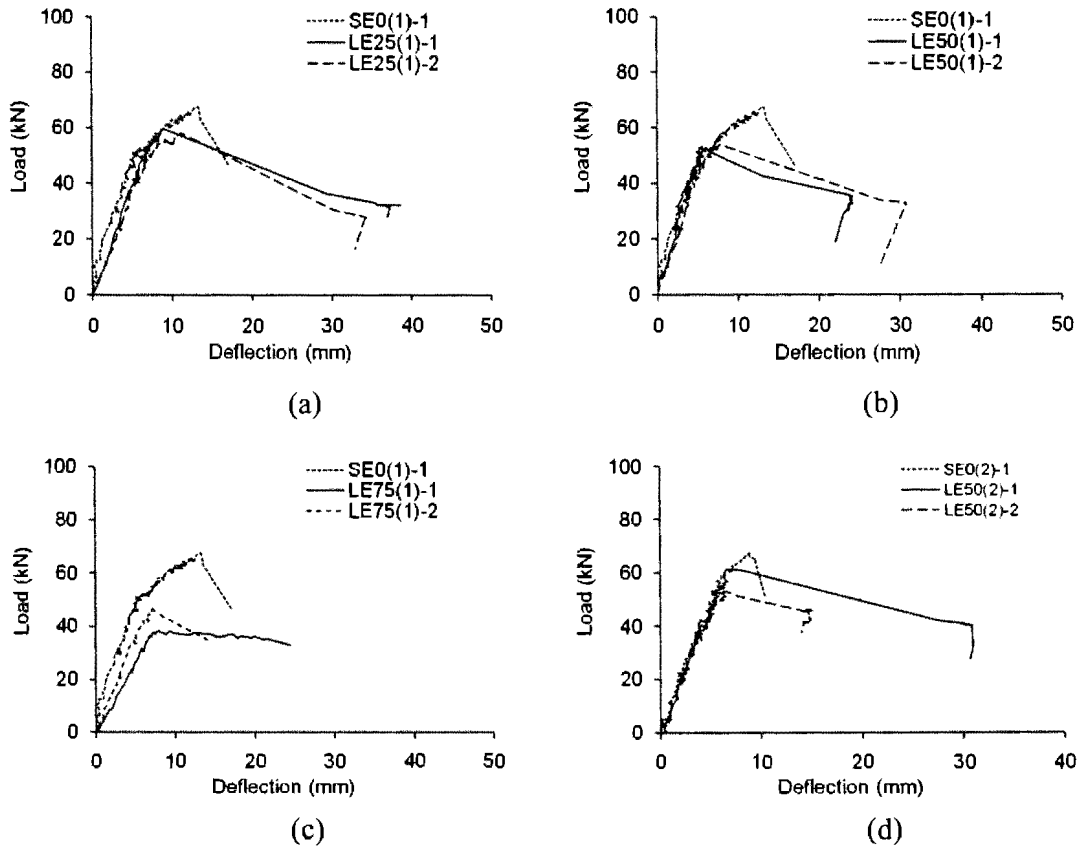
Fig.4.15. Residual load-displacement behavior of long-term beams with CFRP strips: (a) 25% P_u; (b) 50% P_u; (c) 75% P_u; (d) 50% P_u (2 layers of CFRP)

4.5.4. Failure Mode

Table 4.1 compares the failure modes of monotonic, cyclic, and long-term beams. The reference control beam failed due to crushing of the concrete in compression. Beams strengthened with one layer of CFRP strip failed by interfacial failure between the concrete

and NSM CFRP, however beam SE0(2)-1 with two layers of CFRP failed due to debonding of the CFRP at its end [Fig. 4.16]. In spite of using different bonding agents, Beams SC0(1)-1 and SG(1)-1 exhibited similar interfacial failure compared to Beam SE0(1)-1. The interfacial failure can be classified into pure interfacial failure and cohesive shear failure in the adhesive (Szabo and Balazs 2007) where the pure interfacial failure can be identified by the absence of adhesive remained at the FRP surface after failure and the cohesive shear failure can be identified by the presence of adhesive on both FRP and concrete after failure. Due to the application of cyclic load the short-term beams SE0(1)-2 and SE0(2)-2 showed debonding failure except SC0(1)-2 in which cement-grout was used as a bonding agent. All the long-term beams failed due to debonding of the CFRP at its end followed by compression failure of the concrete [Fig. 4.17]. Debonding failure occurred in different ways such as i) between concrete and adhesive; ii) between adhesive and FRP; iii) in the concrete cover near the surface along the weakened layer. A propagation of crack initiating near the end of the CFRP strip towards the loading point was observed during the incremental of loads. Some long-term beams such as LE50(1)-1, LE75(1)-1 and LE75(1)-1 exhibited end debonding with significant interfacial bond deterioration due to application of high magnitude of sustained intensities. Failure of these specimens occurred through the simultaneous separation of CFRP strip and epoxy from the concrete [Fig. 4.17].

4.6. SUMMARY AND CONCLUSIONS

- The beams strengthened with the NSM CFRP strip displayed superior flexural response under monotonic and cyclic loading condition in comparison to the control beam. The failure modes were dominated by the application of cyclic loading and a different failure mode was observed when compared to the monotonic one.

- The effect of sustained intensities was noticeable on the residual load-carrying capacity of the NSM beams. The ultimate capacity decreased with the increase of sustained intensities. A gradual degradation of CFRP strain with respect to time was observed during the constant stress period which indicates the deterioration of interface in between the CFRP strip and adhesive. Debonding failure was also observed when the long-term beam when loaded until failure under a monotonic loading condition.

- Three types of failure were observed in the case of NSM strengthen beams, depending upon different loading conditions. These failures are concrete crushing, interfacial failure and debonding failure.

(a)   (b)
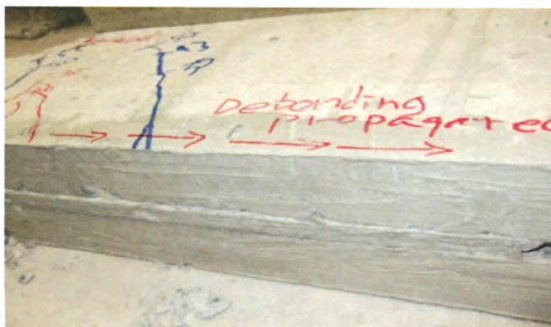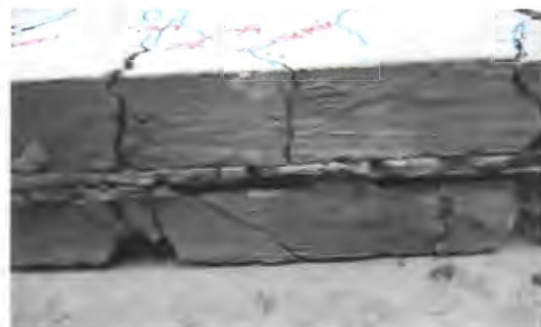
(c)   (d)

Fig.4.16. Failure mode of short-term beams: (a) 1 layer epoxy monotonic; (b) 2 layers epoxy; (c) 1 layer cement-grout; (d) 1 layer geopolymer monotonic

<div align="center">(a)</div>

<div align="center">(b)</div>

<div align="center">(c)</div>

<div align="center">(d)</div>

Fig.4.17. Failure mode of long-term beams: (a) 1 layer epoxy 25%P_u; (b) 1 layers epoxy 50%P_u; (c) 2 layer epoxy 50%P_u; (d) 1 layer epoxy 75%P_u

4.7. REFERENCES

American Concrete Institute (ACI). 2008. Guide for the design and construciton of externally bonded FRP systems for strengthneing concrete structures (ACI-440.2R-08), American Concrete Institute Committee 440, Farmington Hills, MI.

Bakis, C.E., Bank LC, Brown VL, Cosenza E, Davalos JF, Lesko JJ, Machida A, Rizkalla SH, Triantafillou TC .2002. Fiber-reinforced polymer composites for construction—state-of-the-art review. J Compos Constr 6:73–87

Brena, S.F., Bramblett, R.M., Wood, S.L., and Kreger, M.E. 2003. Increasing Flexural Capacity of Reinforced Concrete Beams Using Carbon Fibre-Reinforced Polymer

Composite, American Concrete Institute (ACI), Structural Journal, Vol. 100, No. 1, pp.36-46.

Ceroni, F. 2010. Experimental performances of RC beams strengthened with FRP materials. Construction and Building Materials. 24: 1547-59

Chami, G. A., Thériault, M., Neale, K.W.2009. Creep behaviour of CFRP-strengthened reinforced concrete beams, Construction and Building Materials, Volume 23, Issue 4, Pages 1640-1652

De Lorenzis, L., Nanni, A., and La Tegola, A. 2000. Strengthening of reinforced concrete structures with near surface mounted FRP rods, bibl. International Meeting on Composite Masterials, PLAST 2000, Milan, Italy, May 9-11, p 8.

Firas Al-Mahmoud, Amjad Kreit, Arnaud Castel & Raoul Francois. 2009. Corroded RC beam repaired with near-surface mounted CFRP rods. Concrete Repair, Rehabilitation and Retrofitting II − Alexander et al (eds)© 2009 Taylor & Francis Group, London, ISBN 978-0-415-46850-3
Hassan, T. and Rizkalla, S. 2003. Investigation of Bond in Concrete Structures Strengthened with Near Surface Mounted Carbon Fiber Reinforced Polymer Strips, Journal of Composites for Construction, Vol 7, No. 3, pp. 248-257

Harries, K., and Aidoo, J. 2006. Debonding and fatigue-related strain limits for externally bonded FRP. J. Compos. Constr., 10(1), 87–90.

Harries, K. A., Reeve, B., and Zorn, A. 2007. Experimental evaluation of factors affecting monotonic and fatigue behavior of fiber-reinforced polymer-to-concrete bond in reinforced concrete beams. ACI Struct J., 104(6), 667–674.

Harries, K. A., Zorn, A., Aidoo, J., and Quattlebaum, J. 2006. Deterioration of FRP-to-concrete bond under fatigue loading. Adv. Struct.Eng., 9(6), 779–789.

Hughes Brothers. 2009. Carbon Fiber Reinforced Polymer (CFRP) Tape Aslan 500, Hughes Brothers, Nebraska, USA.

Jung, W. T., Park, H. Y., Park, J. S., Kang, J. Y., and Yoo, Y. J. 2005. Experimental investigation on flexural behavior of RC beams strengthened by NSM CFRP reinforcement. Proc., Int. Symp. On Fiber-Reinforced (FRP) Polymer Reinforcement for Concrete Structures, ACI Symposium Publication, Farmington Hills, Mich., 795–806.

Kim, Y.J., Fam, A., Kong, A., and El-Hacha, R. 2005. Flexural strengthening of RC beams using steel reinforced polymer (SRP) composites, American Concrete Institute (ACI) Special Publication on Fiber Reinforced Polymer Reinforcement for Concrete Structures (SP-230), 1647-1664.

Kim, Y.J. and Heffernan, P.J. 2008b. Fatigue behavior of structures strengthened with fiber reinforced polymers: state-of-the-art, Journal of Composites for Construction, 12(3), 246-256.

Kim, Y.J., Shi, C., and Green, M.F. 2008. Ductility and cracking behavior of prestressed concrete beams strengthened with prestressed CFRP sheets, Journal of Composites for Construction, 12(3), 274-283.

McKenna, J.K. 1993. Post Strengthening of Reinforced Concrete Members Using Fibre Composite Materials, MEng Thesis, Royal Military Collage, Kingston, Canada.

Rosenboom, O., and Rizkalla, S. 2006. "Behavior of prestressed concrete strengthened with various CFRP systems subjected to fatigue loading." J. Compos. Constr., 10(6), 492–502.

Seracino, R, Raizal Saifulnaz, M.R. Oehlers, D.J. 2007. Generic Debonding Resistance of EB and NSM Plate-to-Concrete Joints. Journal of Composites for Construction 11(1): 62-70.

Savoia, M., Ferracutu, B., Mazzotti, C.2005. Creep deformation of fiber reinforced plastics-plated reinforced concrete tensile members. Journal of Composites for Construction 9 (1).

Shin, Y.S., Lee, C. 2003. Flexural behavior of reinforced concrete beams strengthened with carbon fiber-reinforced polymer laminates at different levels of sustained load. ACI Struct;100(2):231–9.

Täljsten, B. and Carolin, A. 2001. Concrete Beams Strengthened with Near Surface Mounted CFRP Laminates, Proceeding of the fifth international conference on fibre reinforced plastics for reinforced concrete structures (FRPRCS-5), Cambridge, UK, 16-18, pp. 107-116

Plevris, N.and Triantafillou, T.C. 1992. Time-dependent behavior of RC members strengthened with FRP laminates. Journal of Structural Engineering, 120(3), 1016–1041.
Zsombor Kálmán Szabó and György L. Balázs.2007. Near surface mounted FRP reinforcement for strengthening of concrete structures. Rperiodica polytechnic. 51/1 33–38 doi: 10.3311

CHAPTER 5. SUMMARY AND CONCLUSIONS

5.1. SUMMARY OF RESEARCH PROGRAM

The major outcomes from the first phase of the research are the time-dependent behavior of FRP composites exposed to both room (25°C) and cold temperature (-30°C). These outcomes will benefit the society through improved application of FRP composites for extended service life in both average (25°C) and cold (-30°C) region environments, where the benefits of using advance composite products over conventional materials can be fully recognized. At the beginning of this thesis an extensive literature review was conducted to determine the current state of knowledge on the topics at hand. Then the wide-ranging description of the workshop was portrait through two phases. Phase I was conducted to find out the combined effect of sustained load and cold temperature on the performance of pultruded GFRP beam. This study looks at the long-term behavior of eight beams under three levels (20%P_u, 40%$P_u$and60%P_u of static capacity) of sustained intensities for a period of 2,000 hours. The effect of sustained load associated with low temperature on the overall strength and failure mode of the samples were analyzed. Phase II was conducted to examine the effect of cyclic and sustained loading on the performance of reinforced concrete beam strengthen with NSM technique. In this case, three levels (20%P_u, 40%$P_u$and60%P_u of static capacity) of sustained loads were applied for a period of 4,000 hours. Loading and unloading was performed as cyclic loading during flexural test at every 10kN load to bring the beam under live load effect. This investigation focused on the load-carrying capacity, strain responses and failure pattern.

5.2. DISCUSSION AND CONCLUSIONS

Based on the results of the research program (Phase I) described in chapter 3, the following conclusions can be made:

- The predicted failure of pultruded GFRP beam was categorized into lateral torsional buckling, flange failure, web buckling, and web shear failure among which lateral torsional buckling was found critical. To preclude the lateral torsional buckling lateral braces were installed and the beams were allowed to fail by flange failure.

- After jacking and transfer operation the experimental strain stabilized and then gradually increased up to 2000 hours. Findley power model was used to predict the variation of strain with time and the experimental result displayed good agreements with theoretical prediction.

- The load-carrying capacity decreased due to application of sustained load. The load-carrying capacity decreased 12% compared to control beam due to application of 60%P_u sustained load in room temperature (25°C).

- The effect of sustained intensities associated with cold temperature (-30°C) was critical on the load-carrying capacity of the pultruded GFRP beam. The variation of load-carrying capacity was insignificant in case of the beam with 20% sustained load in cold temperature when compared to control beam. The beam with 40% and 60% sustained load in cold temperature exhibits 6% and 9% lower load-carrying capacity than that of control beam.

- The parametric study indicates a lower visco-elastic modulus and higher creep strain for the beam in room temperature (25°C) compared to the beam in cold

temperature (-30°C).The contribution of the creep parameter n to the viscoelastic modulus was not noticeable at cold temperature.

- A degradation of modulus and stiffness was observedwith the increase of sustained intensity for all cases.

- The failure modes were independent on the level of sustained intensities. The compression flange of the experimental beams started to buckle first. Then Cracks developed along the web-flange junction on the compression face underneath the top flange. The flange cracks then propagated into the web leading to the final failure of the section. This failure showed a well agreement with the predicted failure.

From the research work (Phase II) presented in Chapter 4, the following conclusions can be drawn:

- The flexural strength increased significantly due to strengthening the reinforced concrete beam using near surface mounted technique with CFRP strip. The application of one layer and two layers CFRP strip increased the strength of control beam about 70% and 77% respectively.

- The types of bonding agents affect the ultimate load-carrying capacity of the NSM beams. Due to application of cement-grout and geopolymer adhesive the ultimate load-carrying capacity reduced about 14% and 20% respectively than that of epoxy adhesive.

- The effect of cyclic loading was not significant on the ultimate strength when compared to the beam with monotonic loading as very few numbers of cycles were applied.

- During the period of sustained loading the CFRP strain decreased with the passes of time which indicates the deterioration of bonding between the CFRP strip and epoxy adhesive. Development of cracks was also observed throughout this stage. This crack growth also depends on the level of sustained intensities.

- The observed failure modes can be categorized into three types such as concrete crushing, interfacial failure and debonding failure.

- The load-carrying capacity decreased with the increase of sustained loading. The beam with $25\%P_u$, $50\%P_u$ and $75\%P_u$ sustained load showed 12.5%, 21.4% and 39.2% decrease in ultimate load-carrying capacity respectively.

- All the beams displayed three stages of load deflection behavior.

- The load-deflection curve of the long-term beam showed less stiff than the benchmark specimen. A degradation of maximum defection was observed with the increase of sustained intensities.

5.3. RECOMMENDATIONS FOR FUTURE WORK

This research program is limited to the time-dependent behavior of FRP composites under different levels of sustained load for structural applications. Further research is needed to investigate the overall performance of these FRP composites.The followings are recommended for future work to be completed in this area:

- A similar program should be carried out in different levels of temperature to investigate the change in materials properties with temperature. Design recommendations should be provided to help practicing engineers.

- Tests need to be executed to study the effect of cyclic load on the pultruded structural member in cold temperature. Fatigue responses at low temperature should be investigated.

- In addition to experimental investigations, a theoretical model should be developed on the time-dependent bond deterioration between NSM FRP strips and concrete substrate.

- In order to gain knowledge on the combined effects of sustained and cyclic loading on a CFRP strengthened concrete beam, advanced modelling should be conducted.

- Future research should be conducted to study the response of epoxy adhesive under cyclic loading.

- To avoid the debonding failure in NSM beams, FRP-adhesive systems need to be improved by using additives or chemical modification in polymer chains. This improvement technique will be important.

APPENDIX A. REPORT CARD FOR AMERICA'S INFRASTRUCTURE

Table A.1. ASCE Report Card 2009(ASCE 2009)

SUBJECT	1988*	1998	2001	2005	2009
Aviation	B-	C-	D	D+	D
Bridges	-	C-	C	C	C
Dams	-	D	D	D	D
Drinking Water	B-	D	D	D-	D-
Energy	-	-	D+	D	D+
Hazardous Waste	D	D-	D+	D	D
Inland Waterways	B	-	D+	D-	D-
Levees	-	-	-	-	D-
Public Parks and Recreation	-	-	-	C-	C-
Rail	-	-	-	C-	C-
Roads	C+	D-	D+	D	D-
Schools	D	F	D-	D	D
Solid Waste	C-	C-	C+	C+	C+
Transit	C-	C	C-	D+	D
Wastewater	C	D+	D	D-	D-
America's Infrastructure G.P.A.	C	D	D+	D	D
Cost to Improve	-	-	$1.3 trillion	$1.6 trillion	$2.2 trillion

APPENDIX B. CREEP PARAMETER FOR COMPOSITE MATERIALS

TABLE B.1. Creep parameter of various composite materials (Structural plastic design manual, ASCE 1987)

	T_{emp} °F	Relative humidity, %	Constants for Findley's Eq. 2.4 [4]					Constants for Eq. 2.17 [3]		
			n dimensionless	ϵ_o in. per in.	ϵ_t in. per in.	c_o psi	c_t psi	r_o 10^6 psi	r_t 10^6 psi	R [6]
Polyethylene [5]	77	50	0.154	0.027	0.0021	585	230	0.0216	0.111	1.9
Polymonochlorotri-fluoroethylene	77	50	0.0872 [1]	0.00810	0.00099	2,600	1,475	0.321	1.490	1.38
Polyvinyl chloride [5]	77	50	0.305	0.00833	0.000079	4,640	1,630	0.557	20.5	1.8
Polystyrene	77	50	0.525	0.048	0.0000041	20,000	650	0.417	158.5	2.03
Melamine/glass fabric laminate [2]	77	50	0.0186	0.00575	0.00575	35,000	35,000	6.09	6.09	1.17
Silicone/glass fabric laminate [2]	77	50	0.0283	0.00203	0.00203	7,800	7,800	1.84	3.84	1.26
Grade C canvas laminate	77	50	0.1183	0.001875	0.001875	4,000	4,000	2.13	2.13	3.06
Parallel laminated paper laminate	77	50	0.114	0.00184	0.002019	6,000	14,000	3.26	6.93	2.12
Glass laminated paper laminate	77	50	0.0763	0.00315	0.001176	12,000	8,000	3.81	6.80	1.67
Asbestos laminate	77	50	0.267	0.00311	0.0001271	4,000	2,400	1.29	18.9	2.37
Polyester-resin, 181 glass fabric	73	50	0.090	0.0034	0.000445	15,000	14,000	4.41	31.5	1.27
Polyester-resin, 181 glass fabric	73	immersed in water	0.710	0.0330	0.000170	80,000	13,000	2.42	76.5	1.33
Polyester-resin, glass fiber mat	73	50	0.190	0.0067	0.0011	8,500	8,500	1.27	7.73	2.27
Epoxy resin, 181 glass fabric	73	50	0.160	0.0057	0.000500	25,000	50,000	4.39	100.0	1.24
Epoxy resin, 181 glass fabric	73	immersed in water	0.220	.025	0.000055	80,000	11,000	1.20	200.0	1.19
Polyester/No. 1000 glass fabric	73	50	0.100	0.0015	0.000220	10,000	8,600	6.67	39.1	1.38
Polyester/No. 1000 glass fabric	73	immersed in water	0.190	0.0280	0.000108	80,000	6,500	2.86	60.2	1.38
Polyester/glass woven roving	73	50	0.200	0.0180	0.00100	40,000	22,000	2.22	22.0	1.91

88

APPENDIX C. SHORT-TERM BEHAVIOR OF GFRP BEAM

C.1 THEORY

The deflection of the GFRP beam (Fig. 3.1) consists of two components such as flexure and shear. The flexural component is readily available in elasticity text books, whereas the shear contribution is not presented in most cases. The following describes the derivation of shear deflection for a beam subjected to different types of loading. According to Timoshenko's beam theory, the slope of deflection induced by shear force may be expressed:

$$\frac{dy}{dx} = \frac{V}{KAG} \tag{C1}$$

The shear modulus of GFRP can be obtained from elastic theory with an orthotropic material factor (i.e., $G = kE/(1 + v)$ where k is the material factor available from the manufacturer; E is the elastic modulus in the fiber direction; and v is the major Poisson's ratio).

C.1.1 Four point bending

Based on Fig. C1, Eq. C1 includes three domains:

$$\frac{dy}{dx} = \frac{1}{KAG} \begin{cases} P/2 \rightarrow 0 \leq x \leq a \\ 0 \rightarrow a \leq x \leq L-a \\ -P/2 \rightarrow L-a \leq x \leq L \end{cases} \tag{C2}$$

$$y = \frac{1}{KAG} \left\{ \begin{array}{l} Px/2 \rightarrow 0 \leq x \leq a \\ C_2 = Px/2 \rightarrow a \leq x \leq L - a \\ -Px/2 + PL/2 \rightarrow L - a \leq x \leq L \end{array} \right.$$

The midspan deflection of the beam due to shear force is given as:

$$\delta_{midspan}^{shear} = y_c = \frac{1}{KAG} \left(\frac{Pa}{2} \right) \tag{C3}$$

The total analytical deflection at midspan including the flexural and shear components is therefore given in Eq. C4:

$$\delta_{midspan} = \frac{Pa(3L^2 - 4a^2)}{48EI} + \frac{Pa}{2KAG} \tag{C4}$$
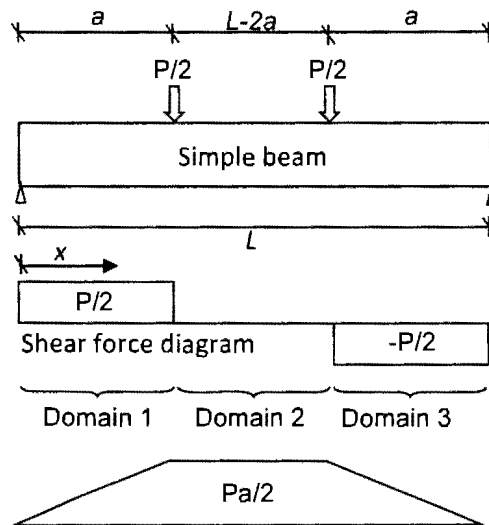
Fig. C1. Four-point bending of beam

90

C.1.2 Four point bending (Equal domain distance)

Based on Fig. C2, Eq. C5 includes three domains:

$$\frac{dy}{dx} = \frac{1}{KAG} \begin{cases} P/2 \to 0 \le x \le L/3 \\ 0 \to L/3 \le x \le 2L/3 \\ -P/2 \to 2L/3 \le x \le L \end{cases} \tag{C5}$$

$$y = \frac{1}{KAG} \begin{cases} Px/2 \to 0 \le x \le L/3 \\ C_2 = PL/6 \to L/3 \le x \le 2L/3 \\ -Px/2 + PL/2 \to 2L/3 \le x \le L \end{cases}$$

The midspan deflection of the beam due to shear force is given as:

$$\delta_{midspan}^{shear} = y_c = \frac{1}{KAG}\left(\frac{PL}{6}\right) \tag{C6}$$
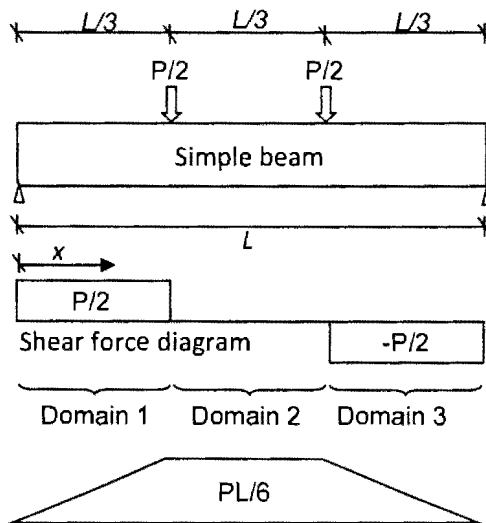
Fig. C2. Four-point bending of beam

The total analytical deflection at midspan including the flexural and shear components is therefore given in Eq. C7:

$$\delta_{midspan} = \frac{Pa(3L^2 - 4a^2)}{48EI} + \frac{PL}{6KAG} \tag{C7}$$

C.1.3 Three point bending

Based on Fig. C3, Eq. C8 includes two domains:

$$\frac{dy}{dx} = \frac{1}{KAG} \begin{cases} P/2 \rightarrow 0 \le x \le L/2 \\ -P/2 \rightarrow L/2 \le x \le L \end{cases} \tag{C8}$$

$$y = \frac{1}{KAG} \begin{cases} Px/2 \rightarrow 0 \le x \le L/2 \\ -Px/2 + PL/2 \rightarrow L/2 \le x \le L \end{cases}$$

The midspan deflection of the beam due to shear force is given as:

$$\delta_{midspan}^{shear} = y_c = \frac{1}{KAG}\left(\frac{PL}{4}\right) \tag{C9}$$

The total analytical deflection at midspan including the flexural and shear components is therefore given in Eq. C10:

$$\delta_{midspan} = \frac{Pa(3L^2 - 4a^2)}{48EI} + \frac{PL}{4KAG} \tag{C10}$$
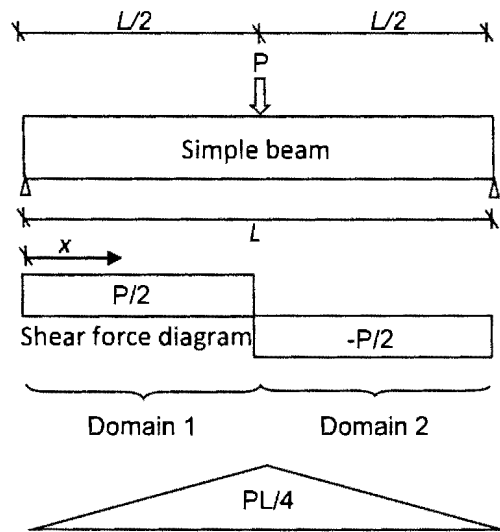
Fig. C3. Three-point bending of beam

C.1.4 Uniform bending

Based on Fig. C4, Eq. C11 includes one domain:

$$\frac{dy}{dx} = \frac{1}{KAG} \left\{ wL/2 - wx \rightarrow 0 \le x \le L \right. \tag{C11}$$

$$y = \frac{1}{KAG} \times \left[wLx/2 - wx^2/2 \right]_{0}^{L/2} \tag{}$$

The midspan deflection of the beam due to shear force is given as:

$$\delta_{midspan}^{shear} = y_c = \frac{1}{KAG} \left(\frac{wL^2}{8} \right) \tag{C12}$$

93

The total analytical deflection at midspan including the flexural and shear components is therefore given in Eq. C13:

$$\delta_{midspan} = \frac{Pa(3L^2 - 4a^2)}{48EI} + \frac{wL^2}{8KAG}$$

(C13)
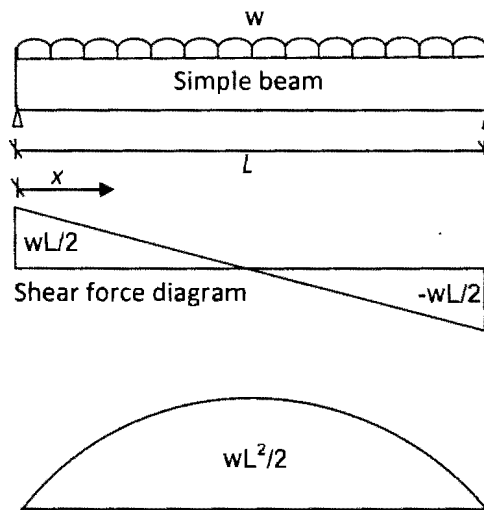
Fig. C4. Uniform bending of beam

C.2 ADDITIONAL PLOTS RELATED TO CHAPTER 3
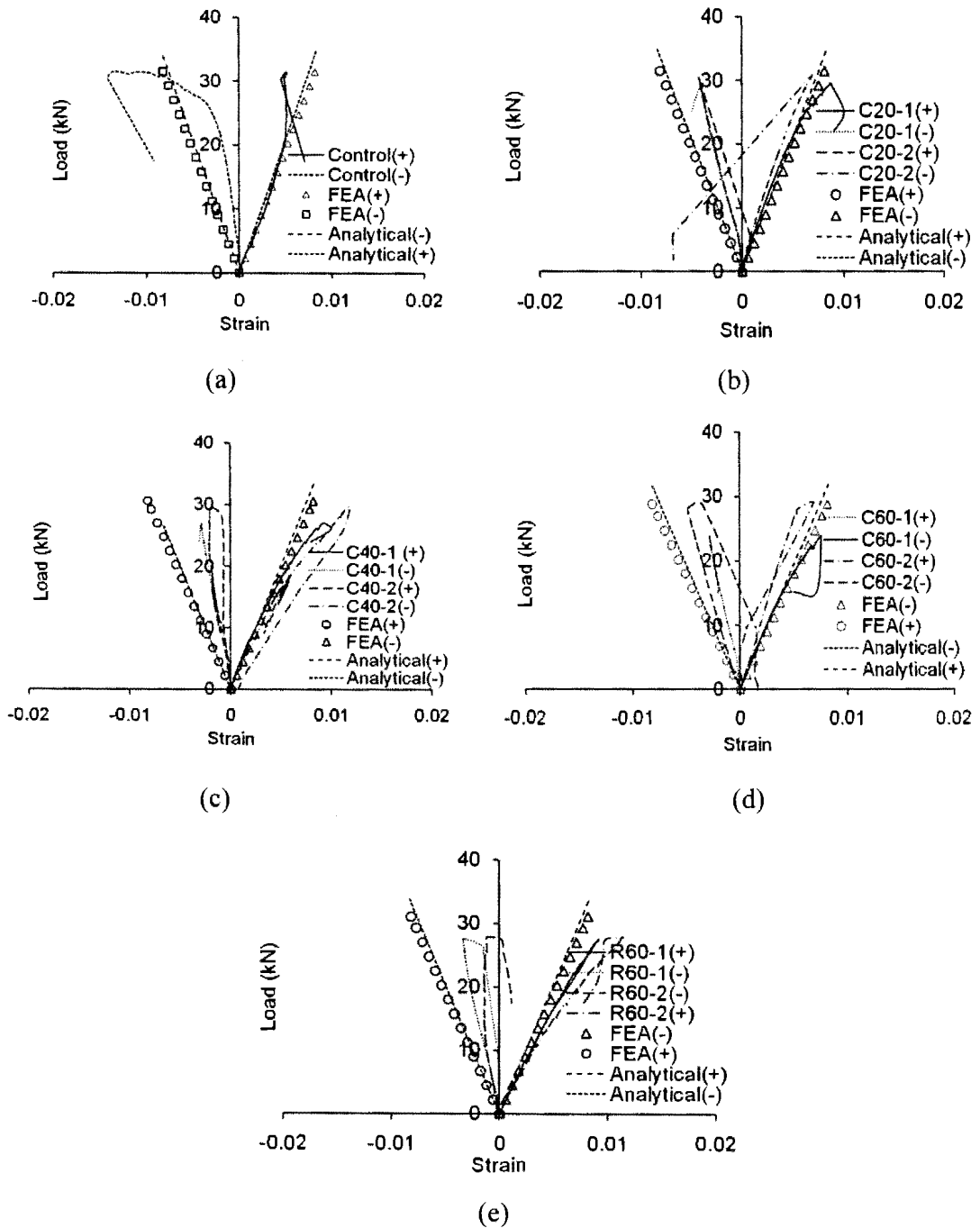
Fig. C5. Load-strain response of GFRP beams: (a) Control at room (25°C); (b) 20%$P_u$at 30°C; (c)40%$P_u$at -30°C; (d) 60%$P_u$at -30°C; (e)60%$P_u$at 25°C (room)
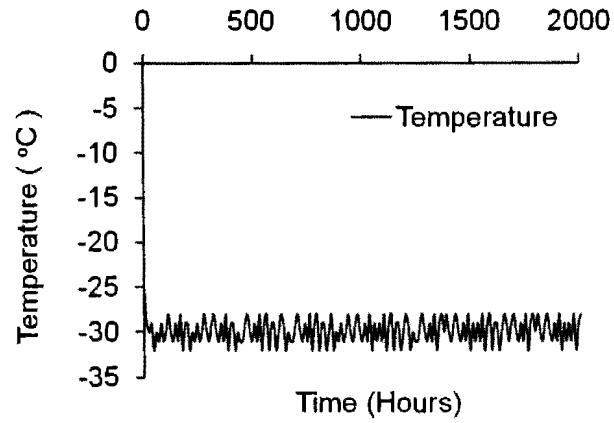
Fig. C6. Variation of temperature during sustained loading
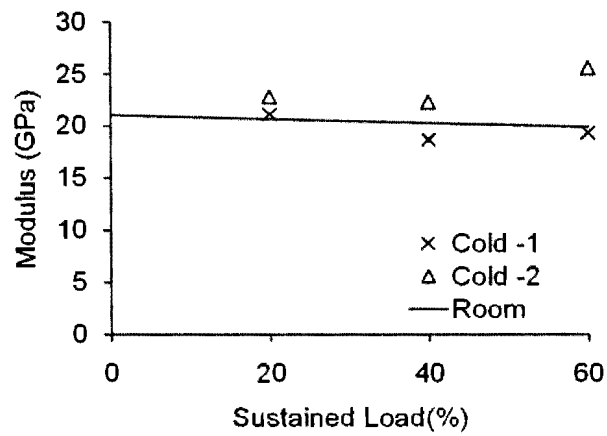
Fig. C7. Modulus degradation with sustained intensities
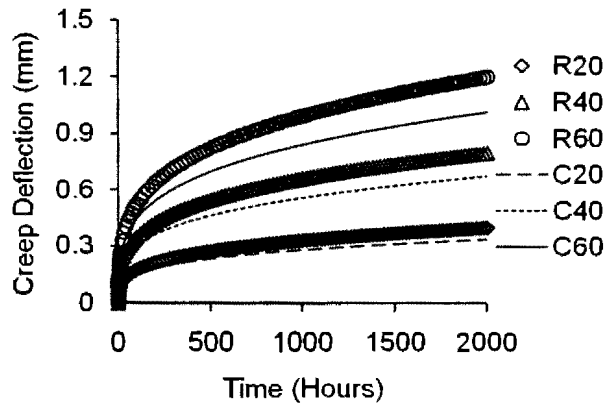
Fig. C8. Creep deflection of GFRP beam

APPENDIX D. RESIDUAL RESPONSE OF NSM BEAM

D.1 ADDITIONAL PLOTS RELATED TO CHAPTER 4
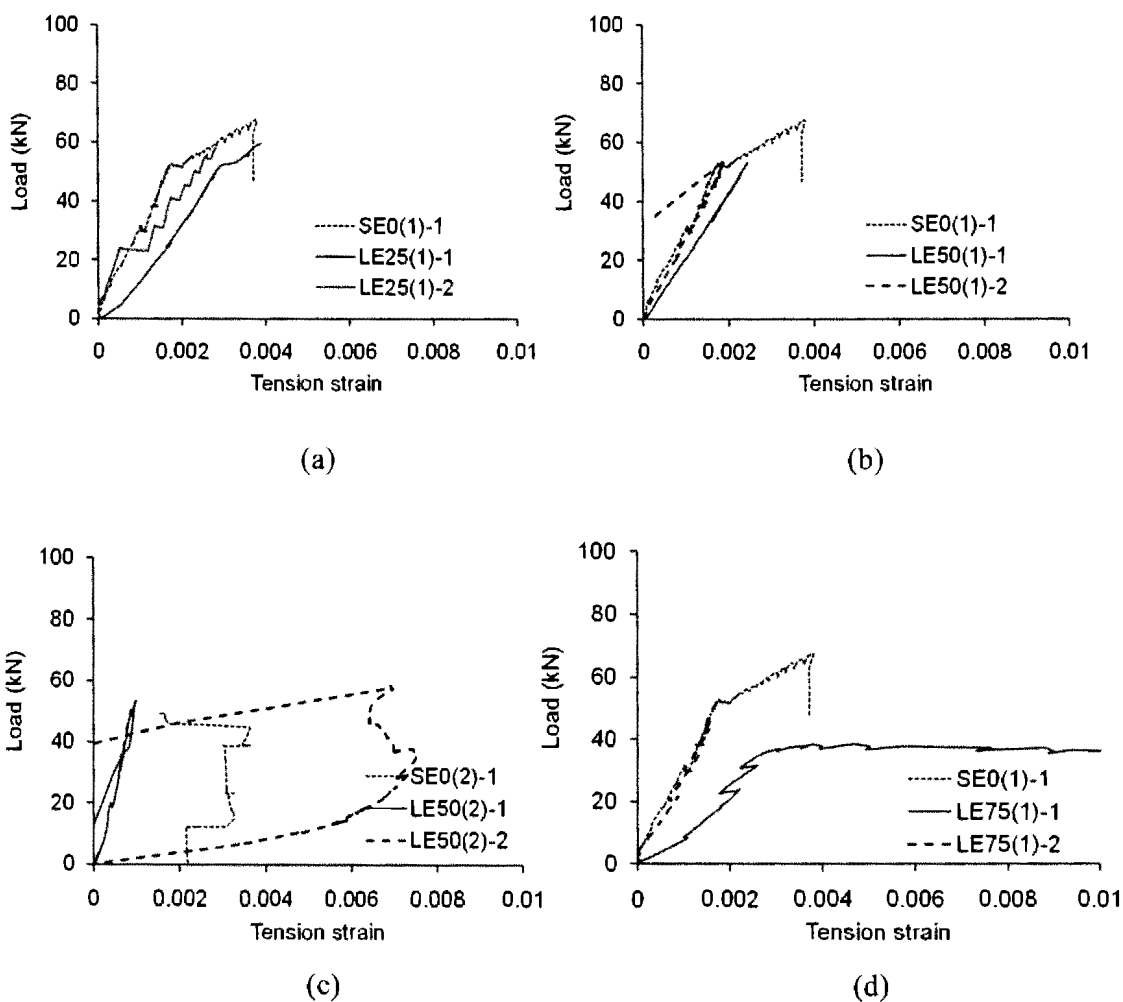
Fig. D1. Load- tension strain response of long-term NSM beams: (a) 25% P_u one layer epoxy; (b)50% $P_u$one layer epoxy; (c) 50%$P_u$two layer epoxy; (e)75%$P_u$one layer epoxy
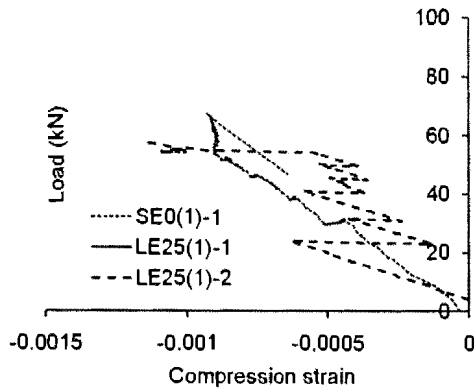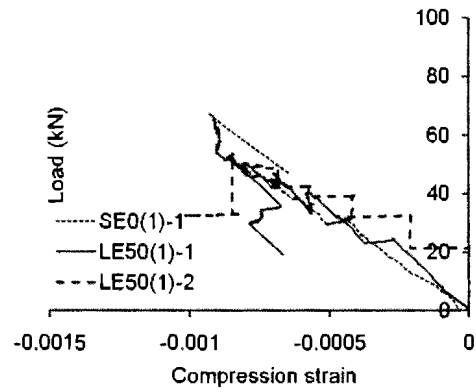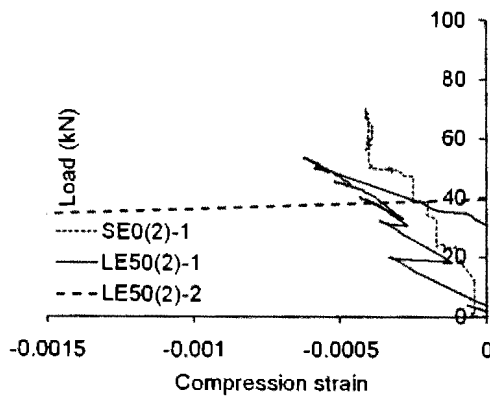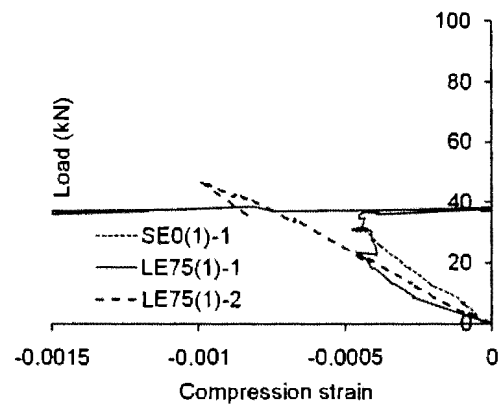
Fig. D2. Load- compression strain response of long-term NSM beams: (a) 25%P_u one layer epoxy; (b)50%P_u one layer epoxy; (c) 50%P_u two layer epoxy; (e)75%P_u one layer epoxy